Supporting Information

Versatile functionalization of the NU-1000 platform by solvent-assisted ligand incorporation

Pravas Deria,[a,†] Wojciech Bury,[a,b,†] Joseph T. Hupp,*[,a] and Omar K. Farha*[,a]

[a] Department of Chemistry, Northwestern University, 2145 Sheridan Road, Evanston, Illinois 60208, United States.

[b] Department of Chemistry, Warsaw University of Technology, Noakowskiego 3, 00-664 Warsaw, Poland.

† These authors contributed equally.

S1. Materials

Reagents and Solvents: Acetone (Macron, 98%), acetonitrile (Macron, 99.8%), dimethyl sulfoxide (DMSO) (Aldrich, 99.8%, anhydrous), *N*,*N*-dimethylformamide (DMF) (Macron, 99.8%), dichloromethane (Macron, 99.0%), deuterated dimethyl sulfoxide (d_6-DMSO) (Cambridge Isotopes, 99%), deuterated sulfuric acid (D_2SO_4) (Cambridge Isotopes, 96-98% solution in D_2O) were used as received without further purification. Compounds **L1-L15**. **L17** and **L18** were purchased from Aldrich, while compound **L16** was obtained from Combi-Blocks; these compounds were used without further purification. Benzyl azide (Alfa Aesar), benzaldehyde (GFS), $CuSO_4{\cdot}5H_2O$ (Aldrich), and (1H,1H,2H,2H-tridecafluorooct-1-yl)phosphonic acid (SynQuest lab) were used as received.

Microcrystalline **NU-1000** was prepared via solvothermal method according to the published procedure.[1]

Secondary structural element: Based on single crystal X-Ray diffraction data it was found that ~20−25% of the mesoporous channels of the **NU-1000** contain a secondary structural element. This secondary element can be represented as $[Zr_6(\mu_3\text{-}O)_4(\mu_3\text{-}OH)_4]_2(TBAPy)_6$ which connects to 12 Zr_6 nodes of the parent framework through six TBAPy ligands. Residual electron density plots from X-Ray diffraction studies and gas sorption studies supported by molecular simulations were inlcuded and disscussed in more detail in the reference 1. It is important to note that complete functionalization upon SALI entails incorporation four carboxylates ligands per node, and results in an idealized-**UiO-66**-like node coordination environment in the **SALI-n** materials; presence of the secondary structural element does not alter the total number of CFGs incorporated into the MOF.

NU-1000 Formulation: The alternative molecular formulation of the Zr_6-based node in **NU-1000** structure would feature bridging oxo and terminal aquo ligands in place of hydroxo ligands. For simplicity, we have referred only to the hydroxo alternative; however both formulations should yield the observed ligand incorporation chemistry.

S2. Instrumentation

Powder X-ray diffraction (PXRD) patterns were recorded on a Rigaku ATXG diffractometer equipped with an 18 kW Cu rotating anode, MLO monochromator, and a high-count-rate scintillation detector (measurements made over a range of $1.5° < 2\theta < 30°$ in 0.05° step width with a 2 deg/min scanning speed). ^{1}H NMR spectra were recorded on Agilent 400 MHz instrument; samples were digested in 10% D_2SO_4/DMSO-d_6. Diffuse reflectance infrared spectra (DRIFTS) were recorded on a Nicolet 7600 FTIR spectrometer equipped with an MCT detector. The spectra were collected in a KBr mixture under N_2 purge (samples were prepared under air); KBr was utilized as the background. Nitrogen isotherms were measured on a Micromeritics TriStar II 3020 at 77 K; for BET surface area analyses we ensured that the two consistency criteria described by Rouquerol et al.[2] and Walton et al.[3] were satisfied. Pore size distribution was calculated using Barrett-Joyner-Halenda (BJH) method with Halsey thickness curve and Kruk-Jaroniec-Sayari correction applied. Thermogravimetric analysis (TGA) was performed on a Mettler Toledo TGA under N2 flow and heated from room temperature to 700 °C (at 10 °C/min).

S3. Synthesis and characterization of SALI-n from NU-1000 ($Zr_6(\mu_3\text{-}OH)_8(OH)_8(TBAPy)_2$)

A 45 mg portion of activated **NU-1000** (0.021 mmol) was loaded into a 5 mL microwave vial (Biotage). Subsequently 3 mL of a 0.07 M solution of CFG (0.21 mmol) in a polar solvent (Table S1) were added to the reaction vial, which was then sealed and heated at 60 ^{0}C for 18-24 h with occasional swirling. The supernatant of the reaction mixture was decanted and the MOF sample was soaked in fresh hot solvent, filtered, washed sequentially with acetone/acetonitrile and dichloromethane (60, 40 and 30 mL each), and finally dried under air.

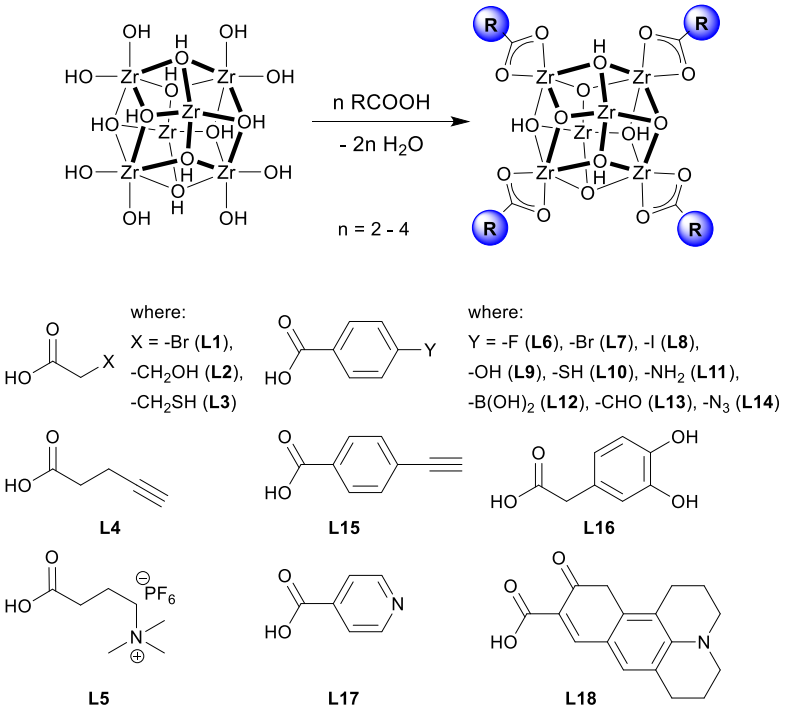

Scheme S1. Synthesis of **SALI-n** via solvent assisted ligand incorporation (SALI) (top). Carboxylic acids (CFGs) used for the functionalization of **NU-1000** (bottom).

Table S1. SALI metrics, BET surface area, pore volume, and BJH pore width of the SALI derived materials.

CFG compound	**SALI-n**	SALI condition[a]	CFG/Zr_6-node	BET [m^2/g]	Pore volume [cm^3/g]	BJH pore width [Å]
NU-1000	**-**	-	-	2315	1.40	30.5
NU-1000/BA	**-**	-	4	1520	0.90	28.0
L1	**11**	MeCN	4	1050	0.65	30.0
L2	**12**	DMF	3.5	1150	0.72	30.5
L3	**13**	DMF	3.5	1730	0.95	30.0
L4	**14**	1:1 DMSO:MeCN	2	1220	0.78	30.0
L5	**15**	MeCN	2	1070	0.74	30.5
L6	**16**	1:4 DMSO:MeCN	4	1025	0.63	29.0
L7	**17**	DMF	4	1180	0.67	27.0
L8	**18**	DMF	4	1430	0.75	26.0
L9	**19**	DMF	3.5	595	0.36	30.0
L10	**20**	DMF	4	1115	0.61	27.5
L11	**21**	DMF	2.5	1160	0.67	28.5
L12	**22**	DMF	3	1245	0.69	28.5
L13	**23**	DMF	3	1240	0.67	27.0
L14	**24**	DMF	4	1750	1.05	30.0
L15	**25**	1:1 DMSO:MeCN	3	1580	0.89	30.0
L16	**26**	MeCN	4	1010	0.63	28.5
L17	**27**	DMF	3.8	1455	0.78	28.0
L18	**28**	DMF	2	1415	0.92	28.5

Characterization data:
1.

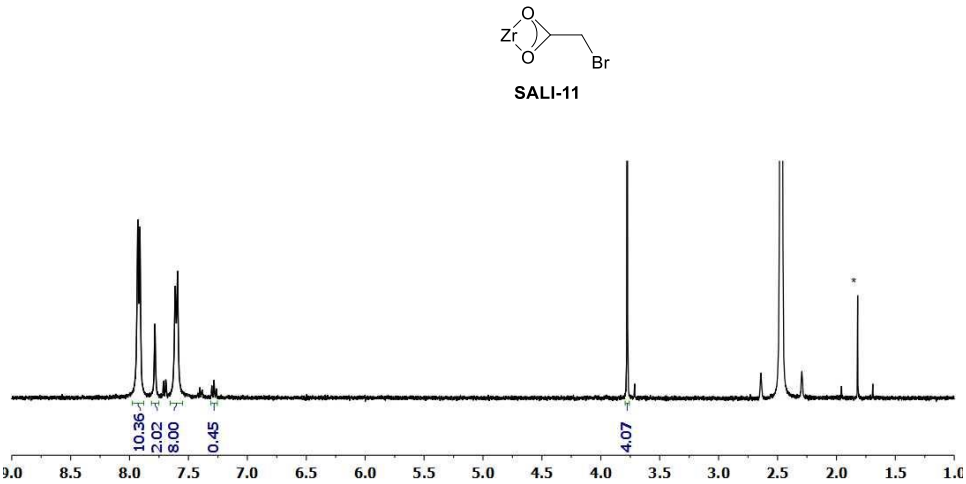

Figure S1. ^{1}H NMR of **SALI-11**. Solvent (MeCN) peak is marked with *.

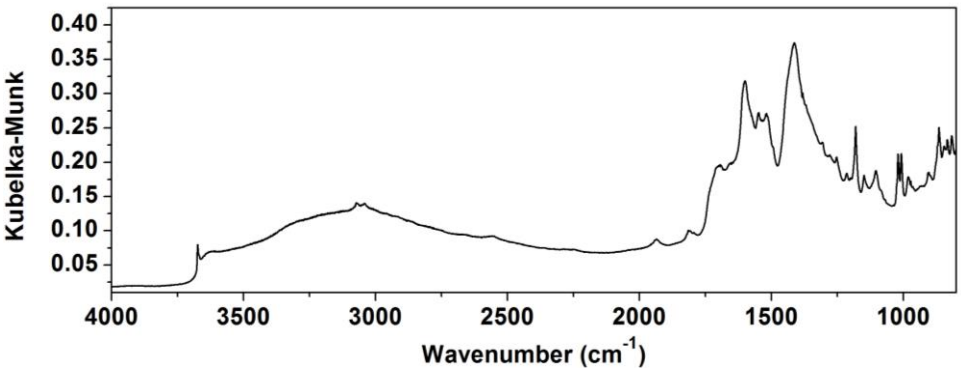

Figure S2. DRIFTS of **SALI-11**.

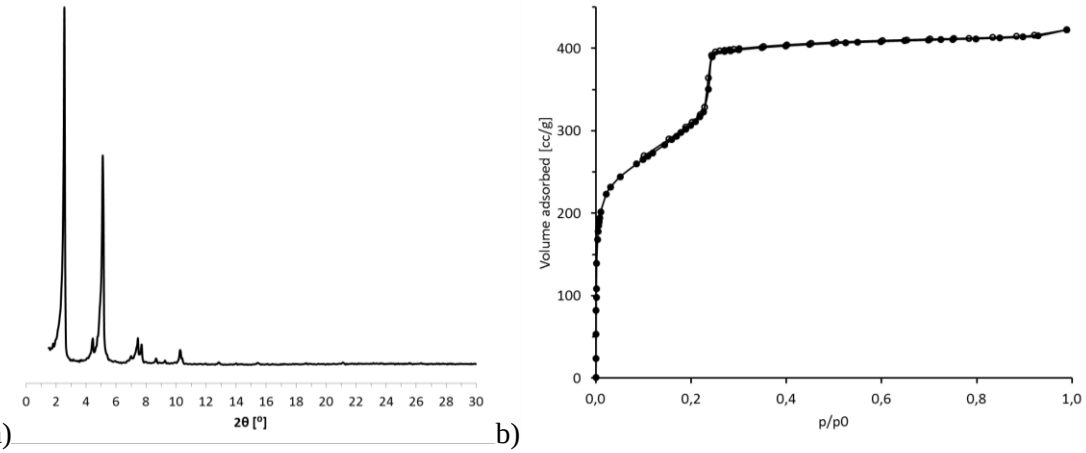

Figure S3. a) PXRD pattern of **SALI-11**, b) N_2 sorption isotherm of **SALI-11**.

2.

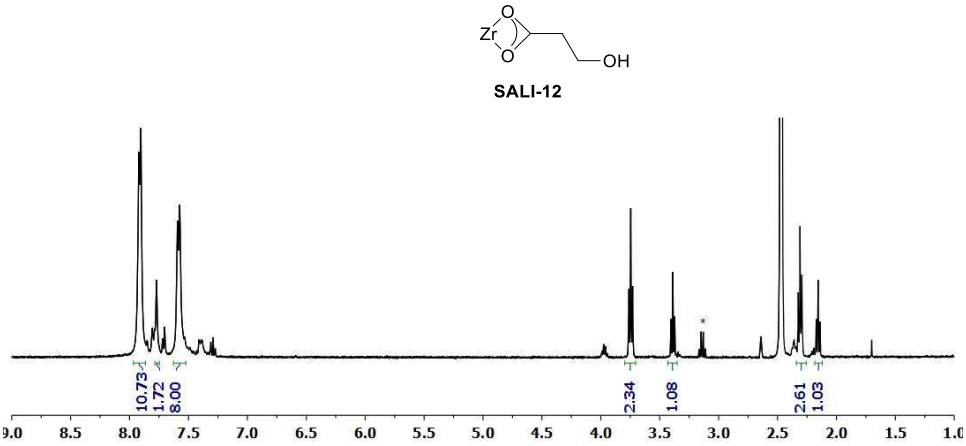

Figure S4. ^{1}H NMR of **SALI-12**. Solvent (ether) peak is marked with *.

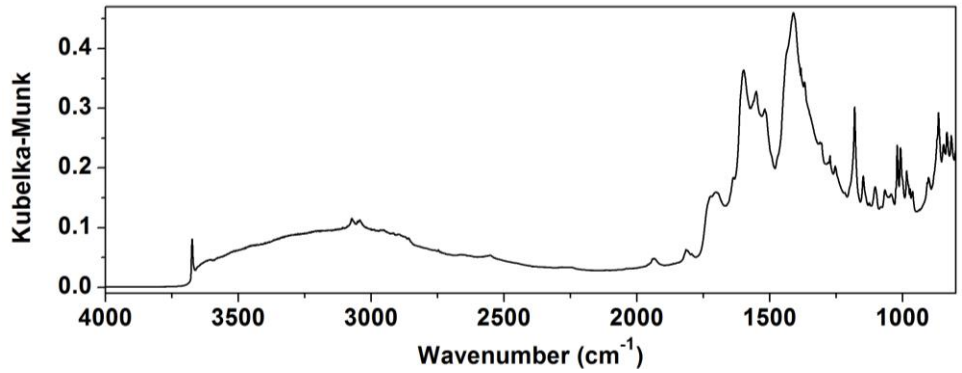

Figure S5. DRIFTS of **SALI-12**.

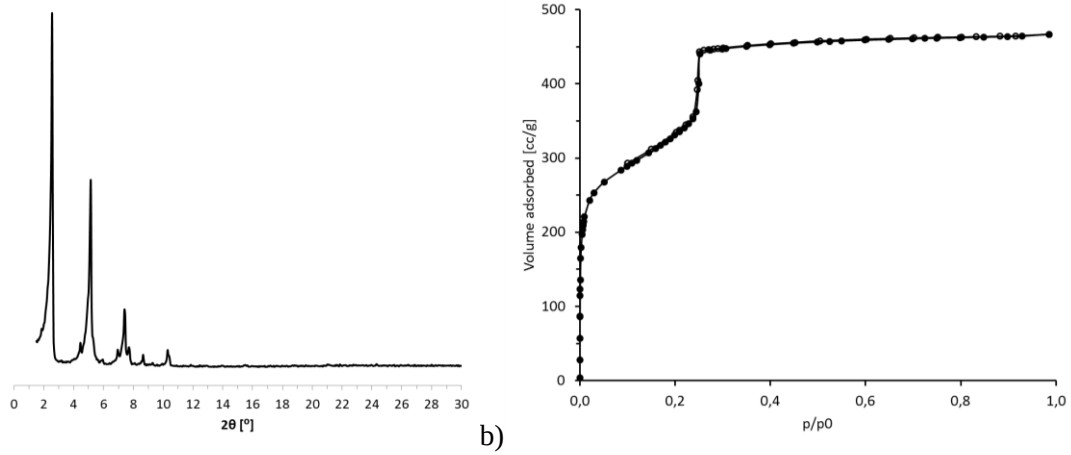

Figure S6. a) PXRD pattern of **SALI-12**, b) N_2 sorption isotherm of **SALI-12**.

3.

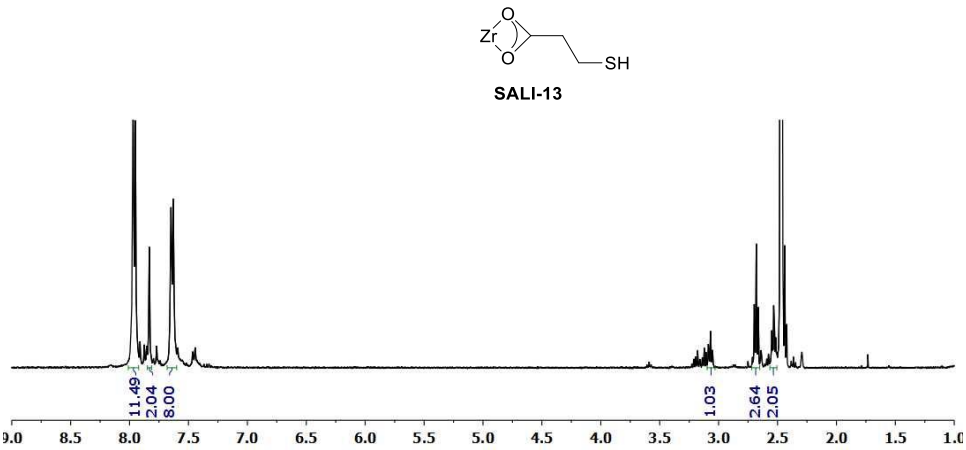

Figure S7. ^{1}H NMR of **SALI-13**.

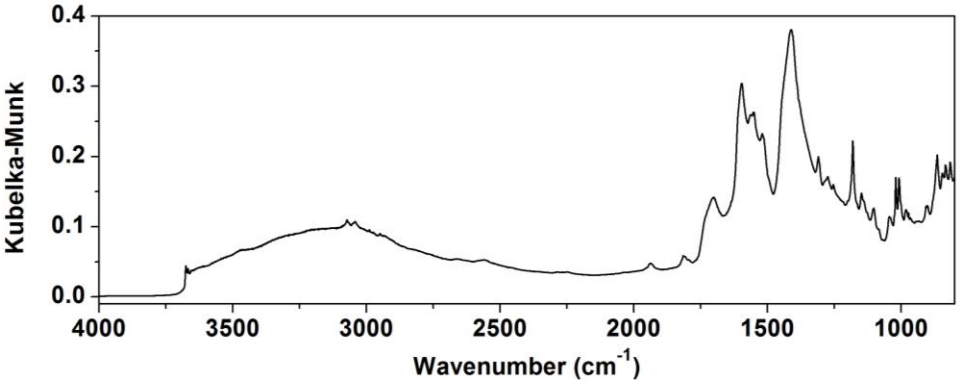

Figure S8. DRIFTS of **SALI-13**.

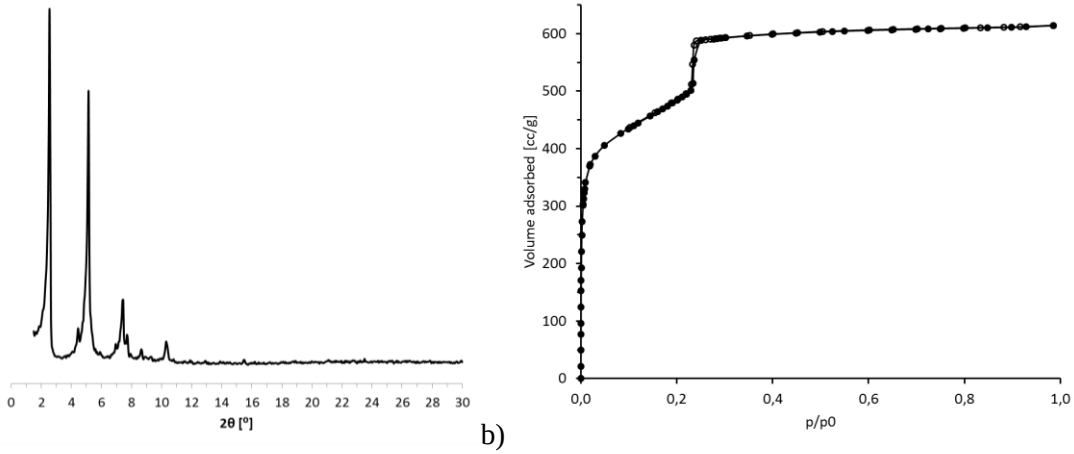

a) b)

Figure S9. a) PXRD pattern of **SALI-13**, b) N_2 sorption isotherm of **SALI-13**.

4.

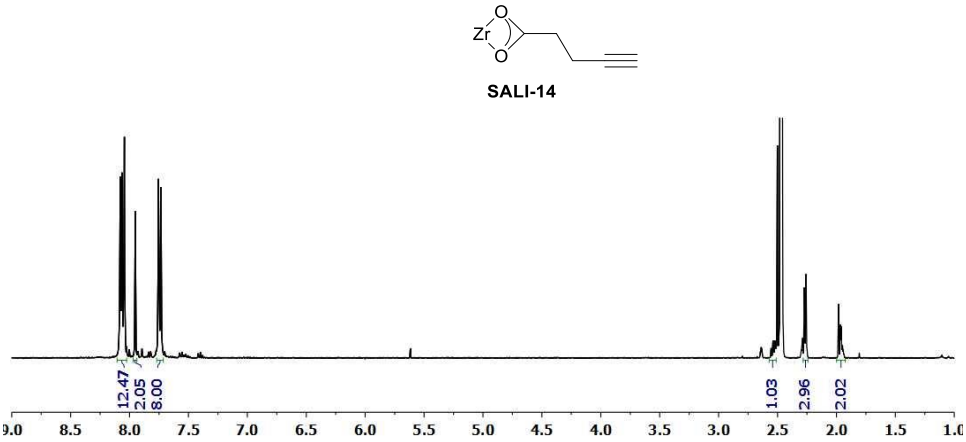

Figure S10. ^{1}H NMR of **SALI-14**.

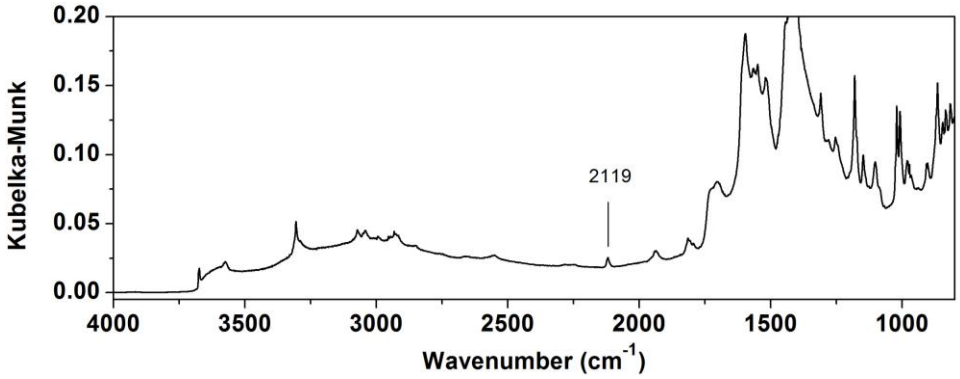

Figure S11. DRIFTS of **SALI-14**. Note the ethyne stretching at 2119 cm^{-1}.

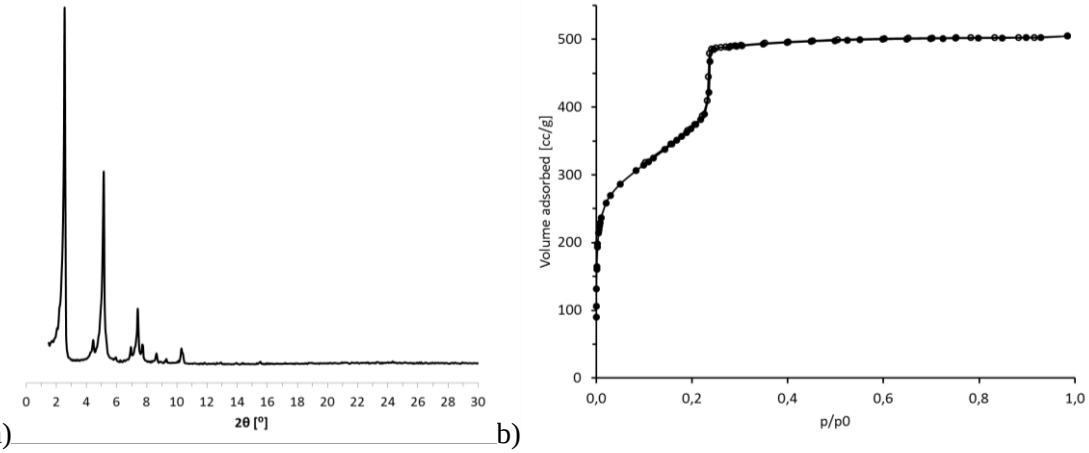

Figure S12. a) PXRD pattern of **SALI-14**, b) N_2 sorption isotherm of **SALI-14**.

5.

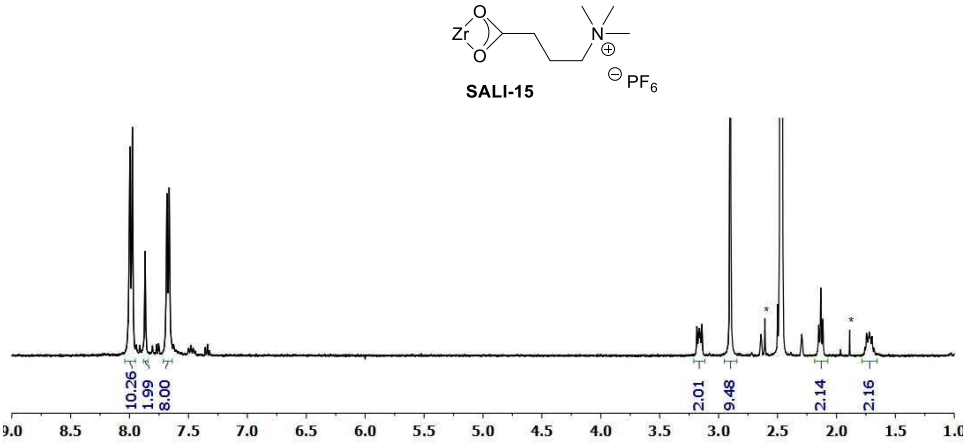

Figure S13. ^{1}H NMR of **SALI-15**. Solvent (DMF, MeCN) peaks are marked with *.

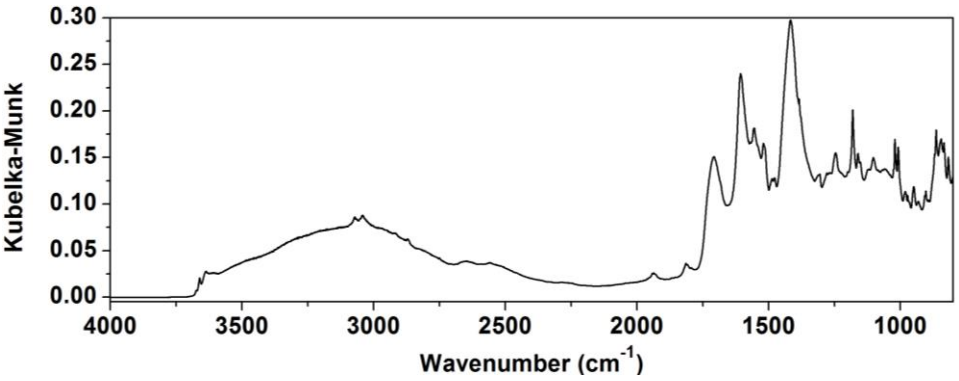

Figure S14. DRIFTS of **SALI-15**.

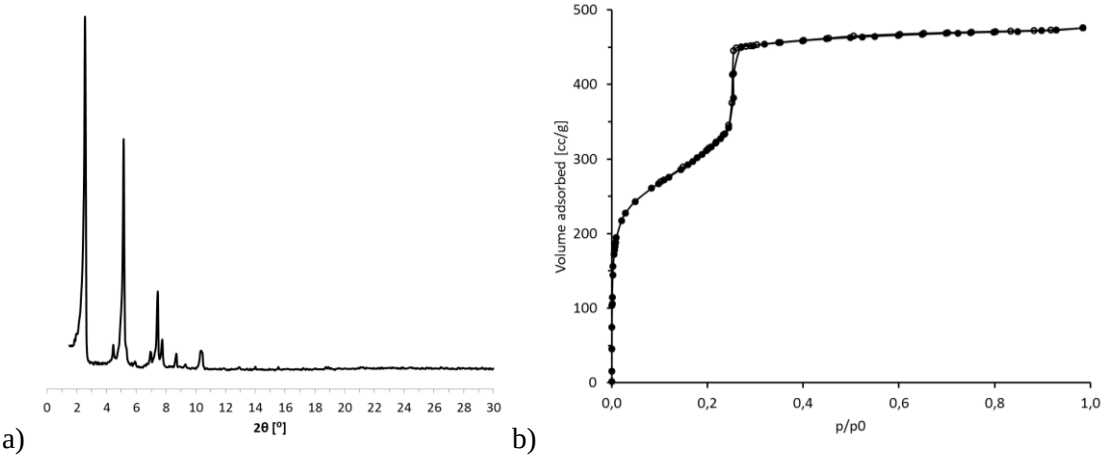

a) b)

Figure S15. a) PXRD pattern of **SALI-15**, b) N_2 sorption isotherm of **SALI-15**.

6.

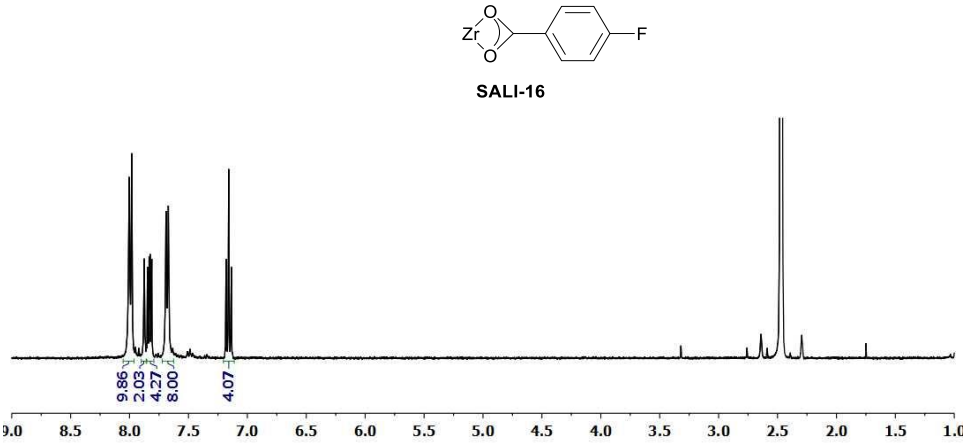

Figure S16. ^{1}H NMR of **SALI-16**.

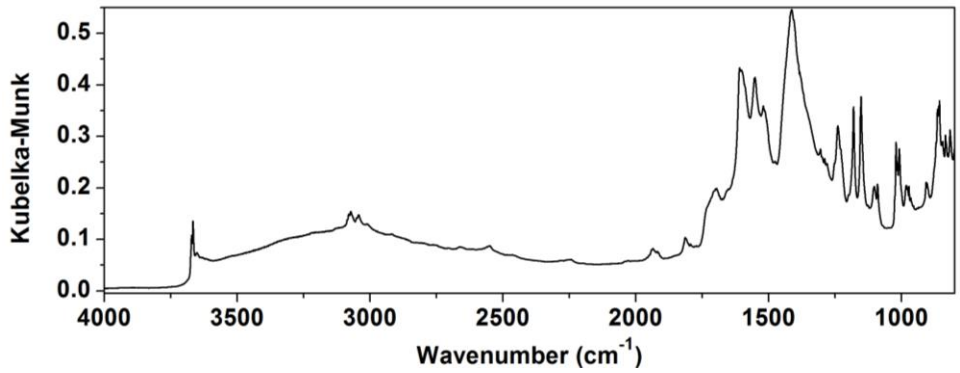

Figure S17. DRIFTS of **SALI-16**.

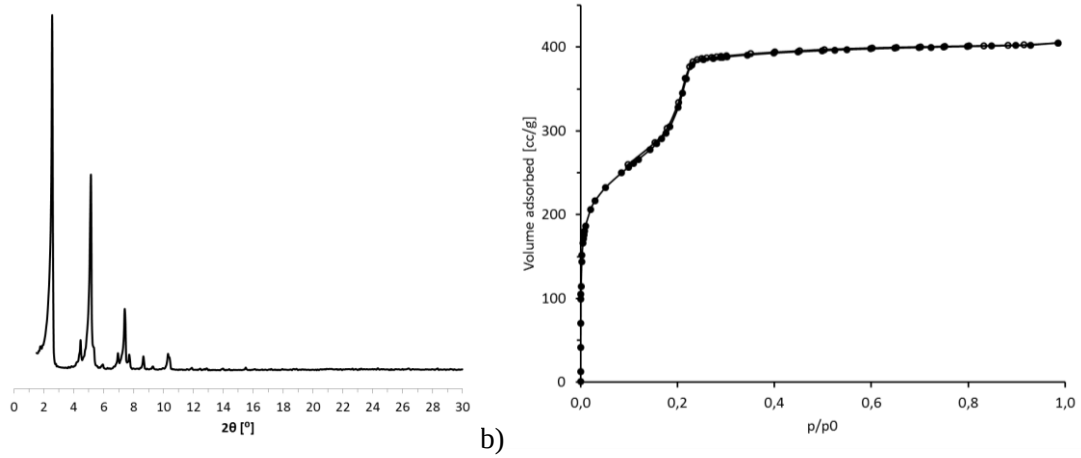

a) b)

Figure S18. a) PXRD pattern of **SALI-16**, b) N_2 sorption isotherm of **SALI-16**.

7.

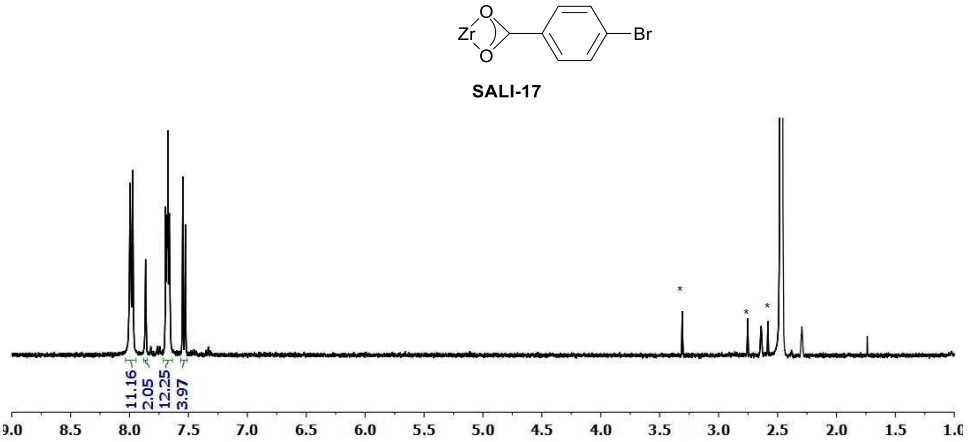

Figure S19. ^{1}H NMR of **SALI-17**. Solvents (DMA, DMF) peaks are marked with *.

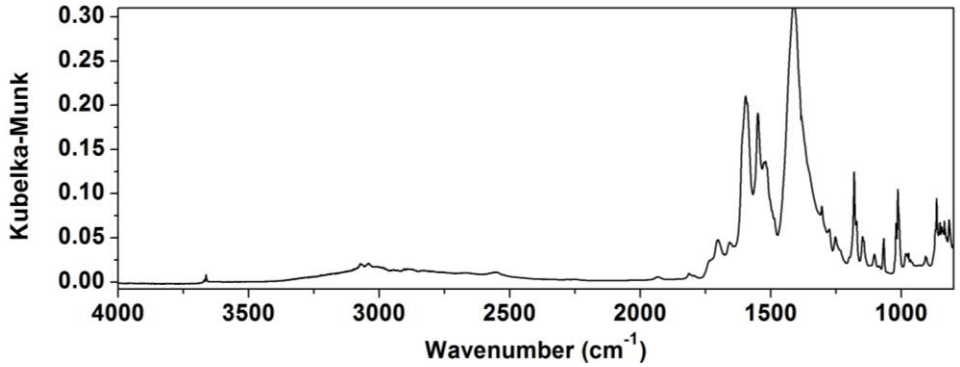

Figure S20. DRIFTS of **SALI-17**.

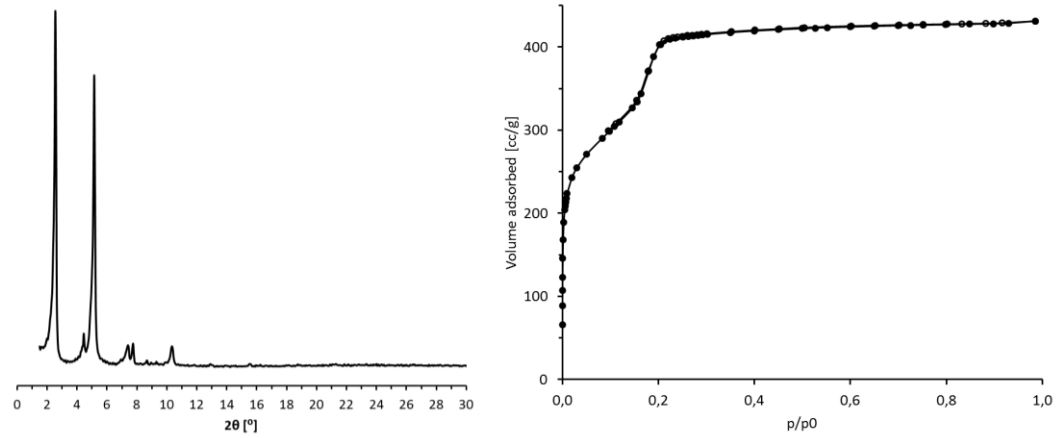

Figure S21. a) PXRD pattern of **SALI-17**, b) N_2 sorption isotherm of **SALI-17**.

8.

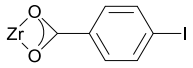

SALI-18

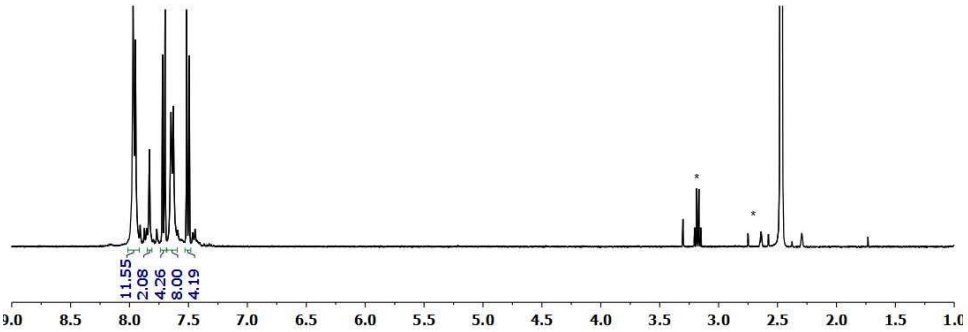

Figure S22. ^{1}H NMR of **SALI-18**. Solvent (ether, DMF) peaks are marked with *.

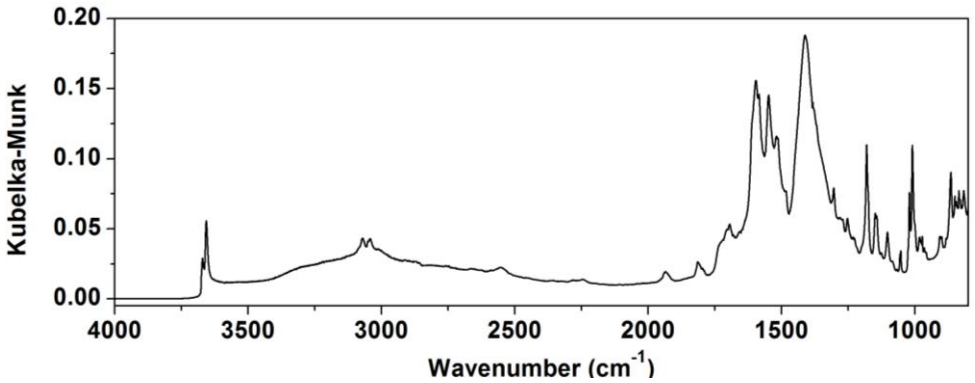

Figure S23. DRIFTS of **SALI-18**.

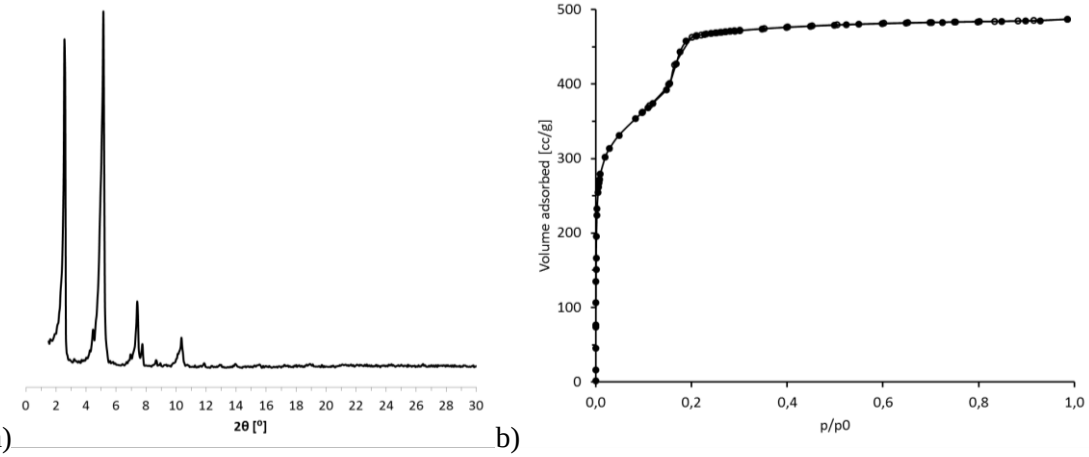

a) b)

Figure S24. a) PXRD pattern of **SALI-18**, b) N_2 sorption isotherm of **SALI-18**.

9.

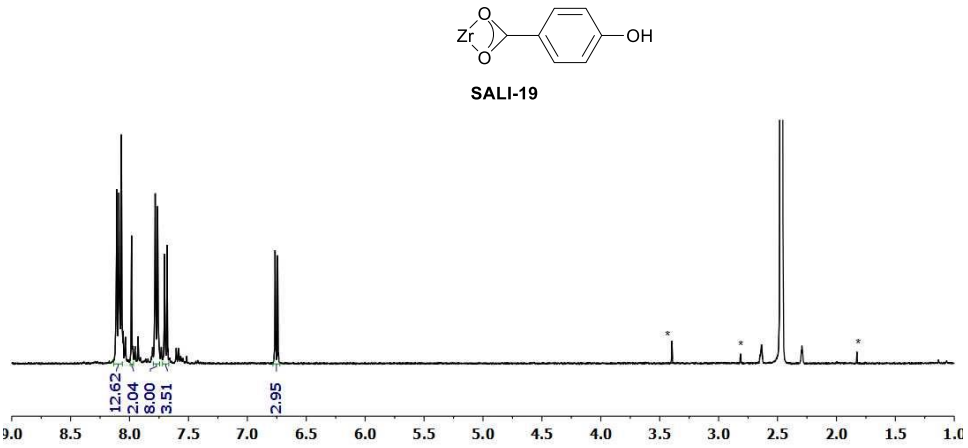

Figure S25. ^{1}H NMR of **SALI-19**. Solvents peaks are marked with *.

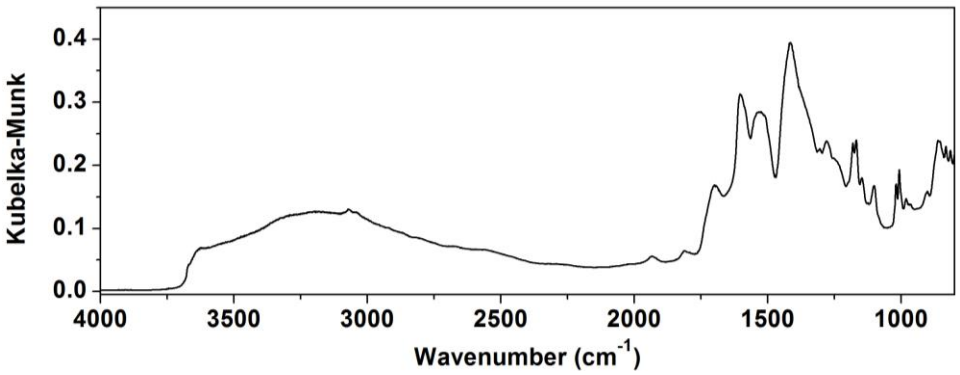

Figure S26. DRIFTS of **SALI-19**.

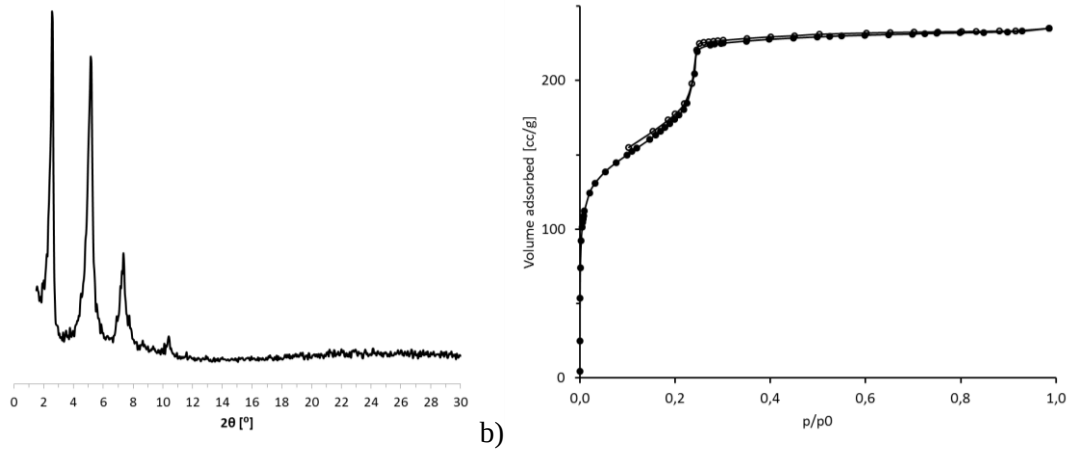

a) b)

Figure S27. a) PXRD pattern of **SALI-19**, b) N_2 sorption isotherm of **SALI-19**.

10.

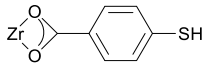

SALI-20

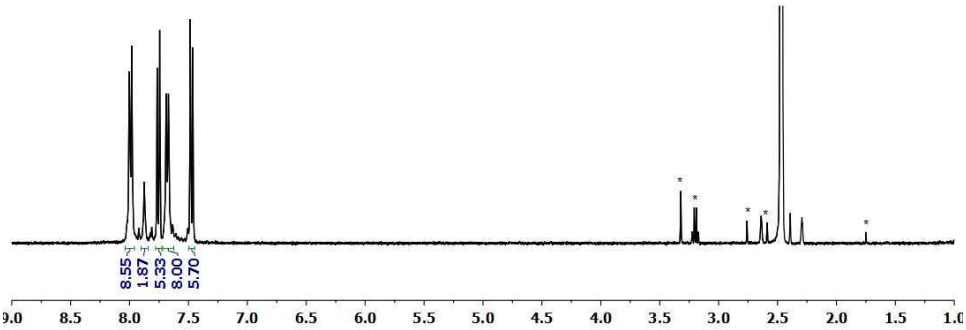

Figure S28. ^{1}H NMR of **SALI-20**. Solvent peaks are marked with *.

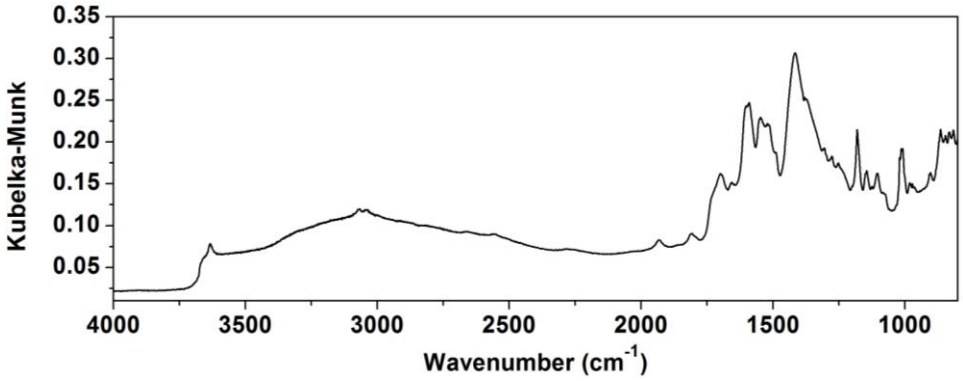

Figure S29. DRIFTS of **SALI-20**.

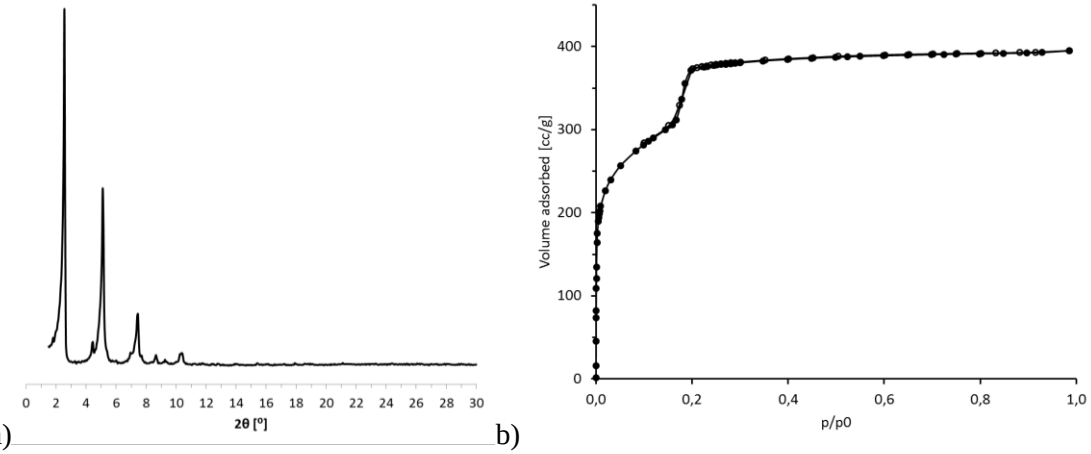

Figure S30. a) PXRD pattern of **SALI-20**, b) N_2 sorption isotherm of **SALI-20**.

11.

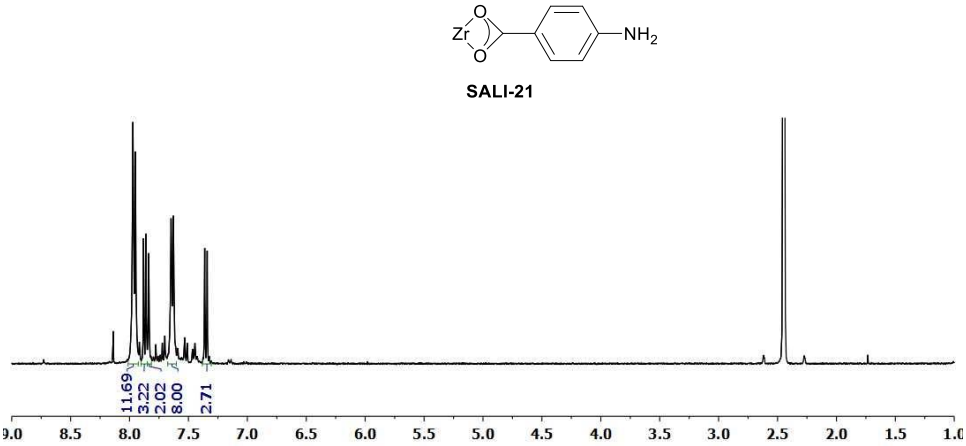

Figure S31. ^{1}H NMR of **SALI-21**.

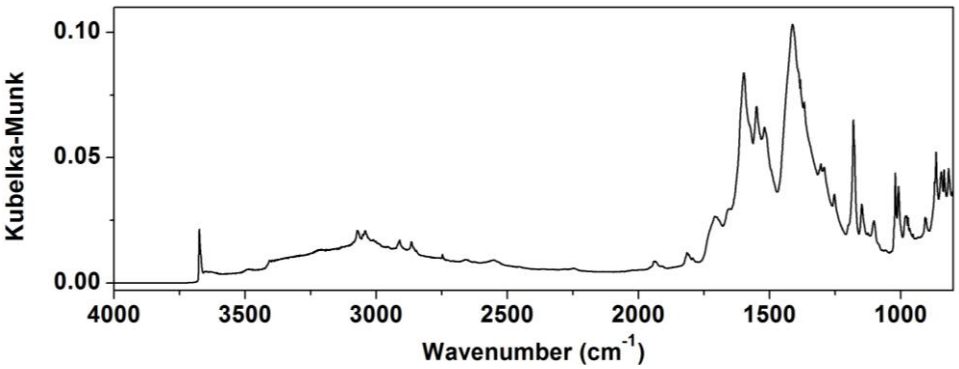

Figure S32. DRIFTS of **SALI-21**.

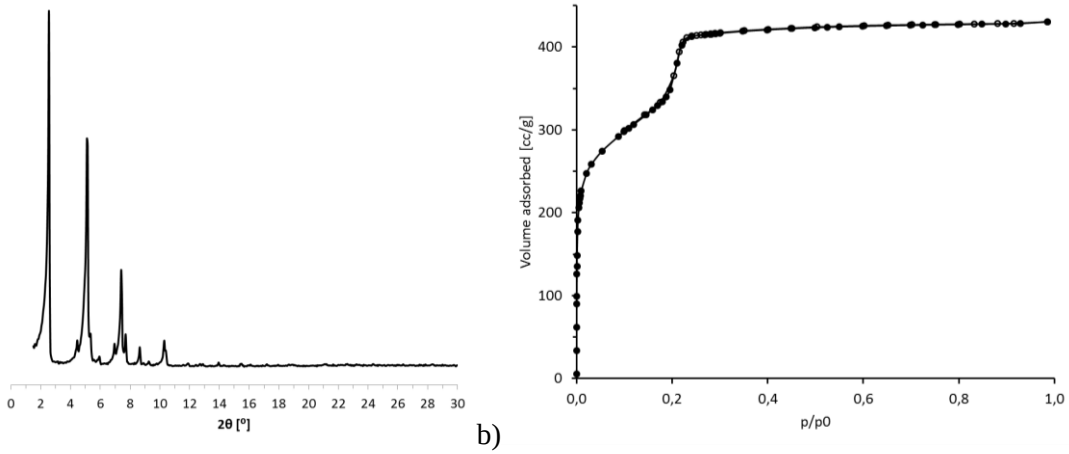

a) b)

Figure S33. a) PXRD pattern of **SALI-21**, b) N_2 sorption isotherm of **SALI-21**.

12.

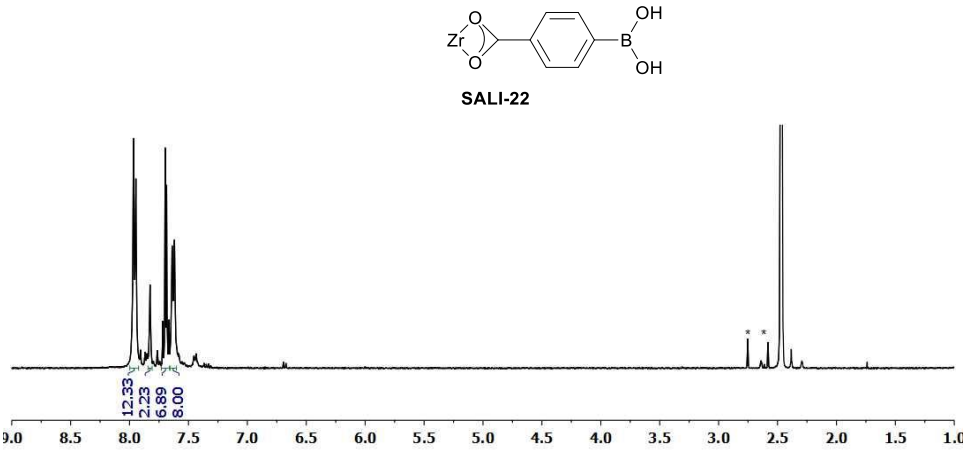

Figure S34. ^{1}H NMR of **SALI-22**. Solvent (DMF) peaks denoted with *.

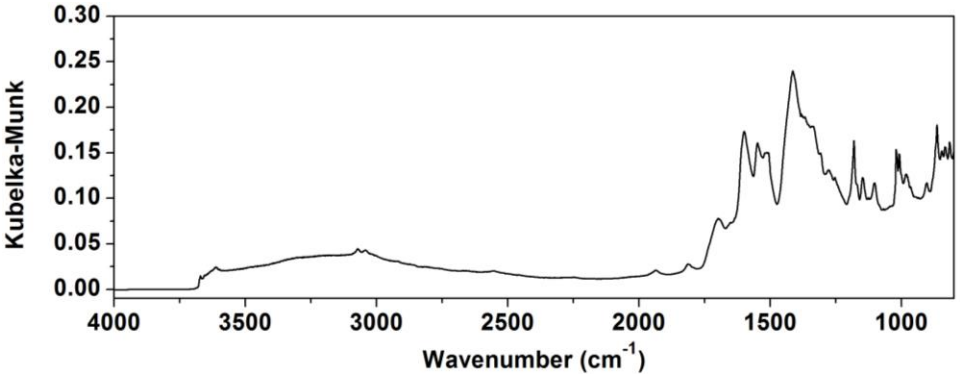

Figure S35. DRIFTS of **SALI-22**.

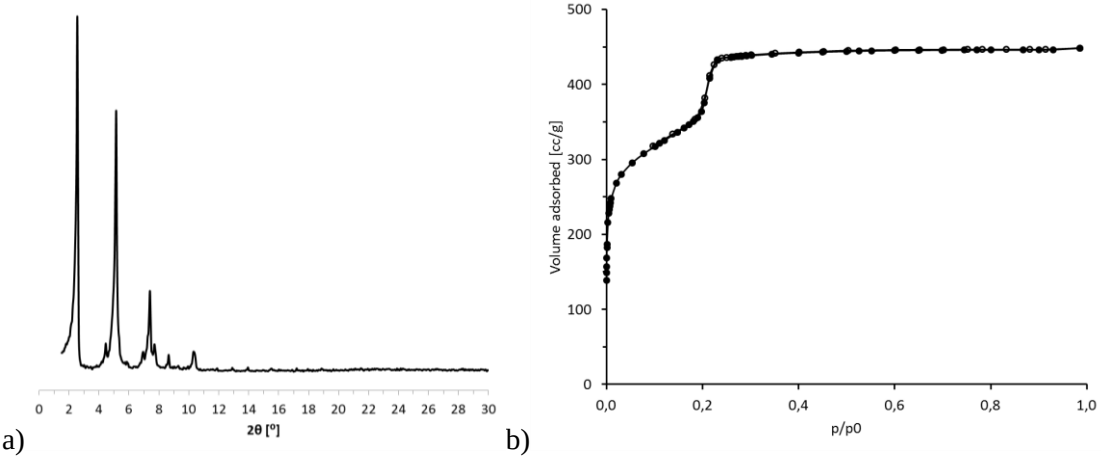

a) b)

Figure S36. a) PXRD pattern of **SALI-22**, b) N_2 sorption isotherm of **SALI-22**.

13.

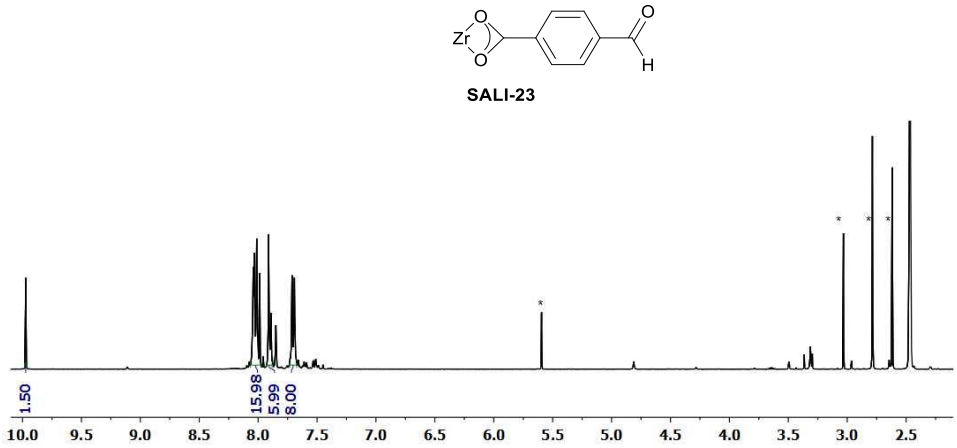

Figure S37. ^{1}H NMR of **SALI-23**. Solvents peaks are denoted with *.

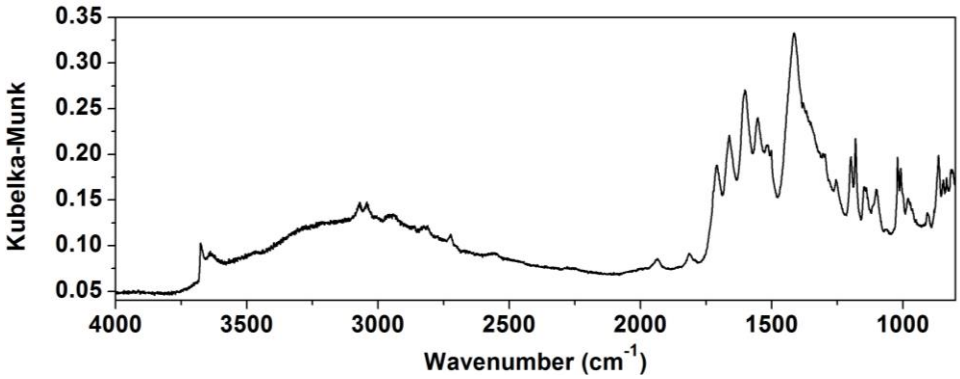

Figure S38. DRIFTS of **SALI-23**.

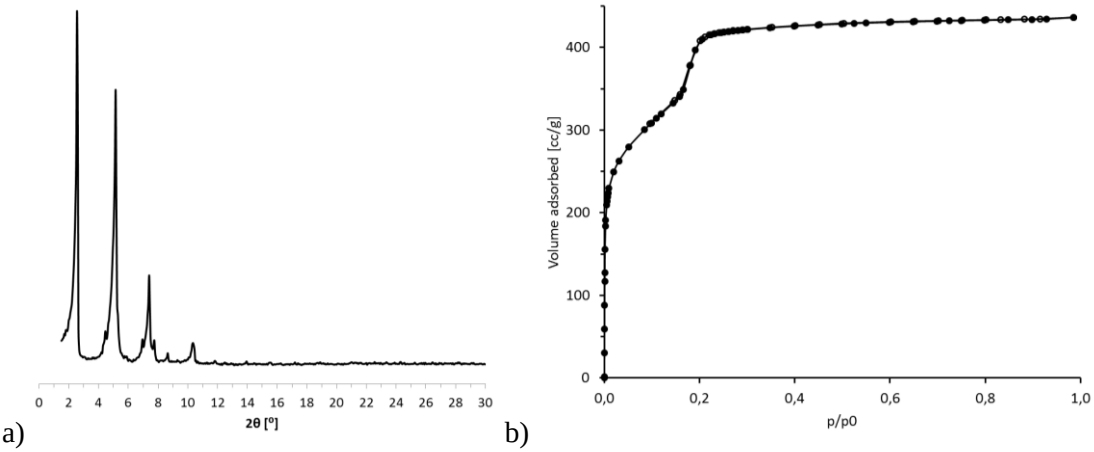

Figure S39. a) PXRD pattern of **SALI-23**, b) N_2 sorption isotherm of **SALI-23**.

14.

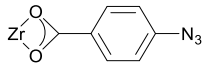

SALI-24

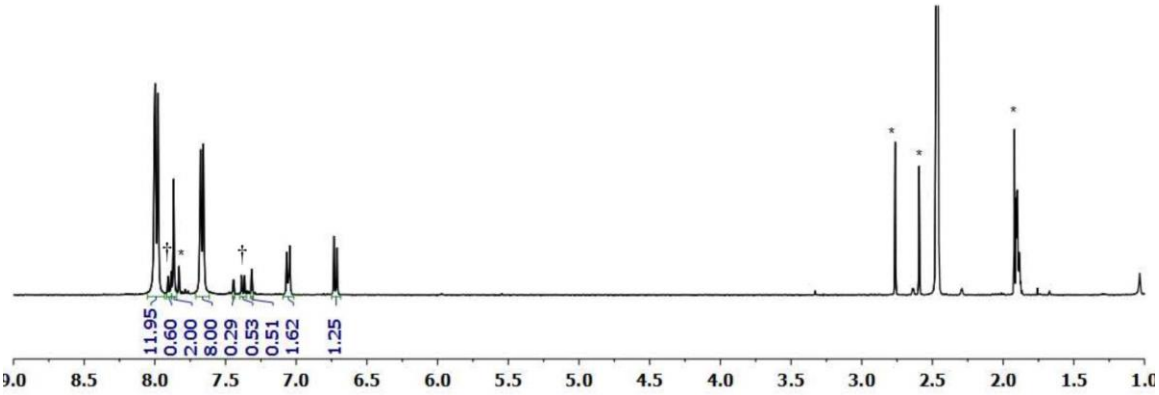

Figure S40. ^{1}H NMR of **SALI-24**. Peaks for 4-aminobenzoic acid (see Figure S-31 for **SALI-21**), formed during acid (D_2SO_4) decomposition of the azide (**L14** in **SALI-24**) for NMR experiment, are marked with †. Solvents (DMF, MeCN) peaks are denoted with *.

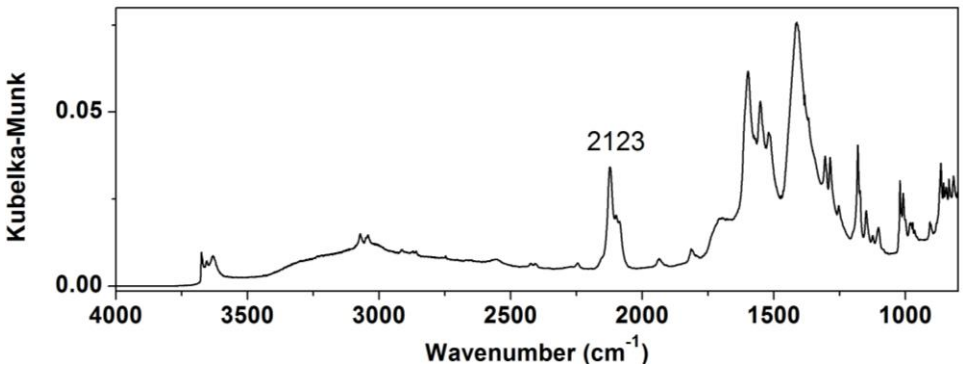

Figure S41. DRIFTS of **SALI-24**.

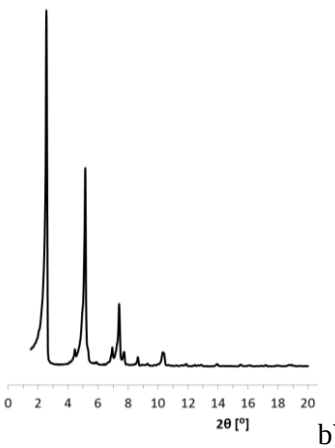

a)

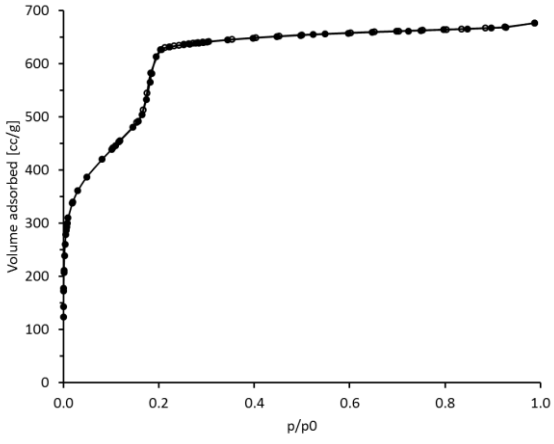

b)

Figure S42. a) PXRD pattern of **SALI-24**, b) N_2 sorption isotherm of **SALI-24**.

15.

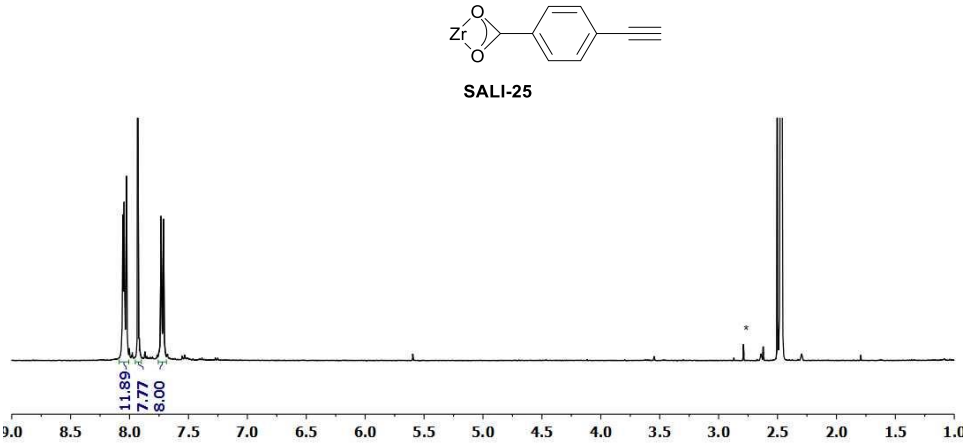

Figure S43. ^{1}H NMR of **SALI-25**. Solvent (DMF) peak is marked with *.

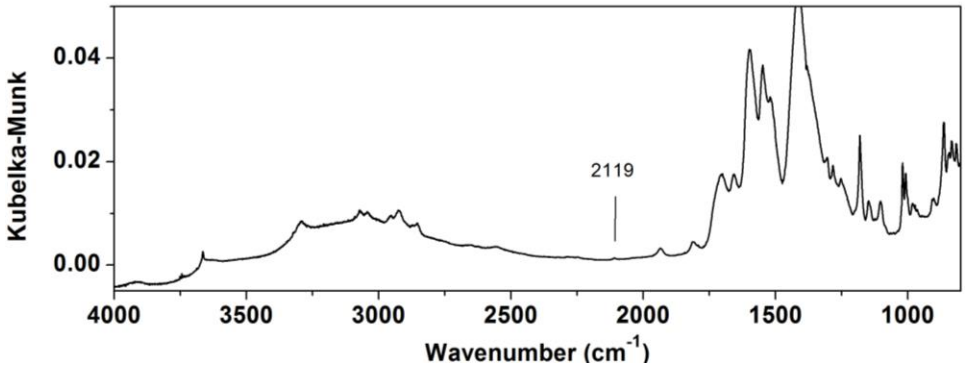

Figure S44. DRIFTS of **SALI-25**.

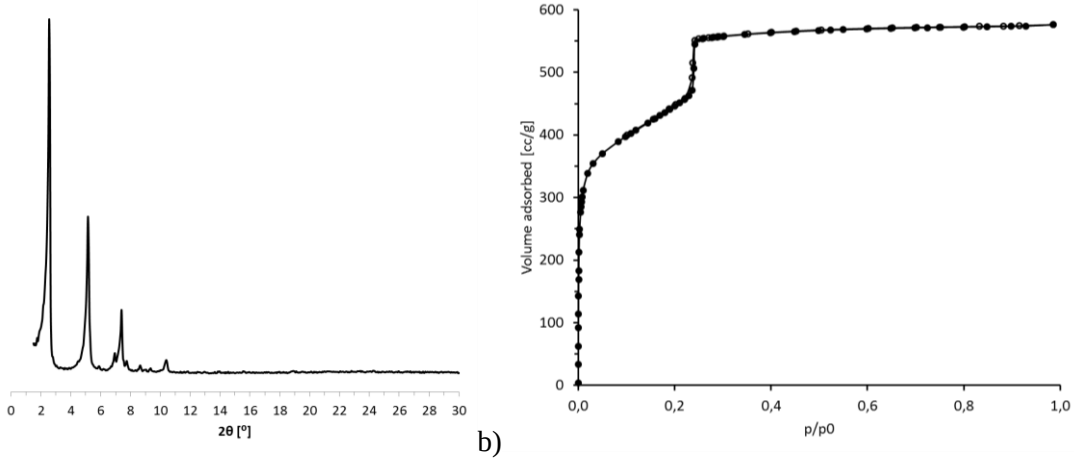

Figure S45. a) PXRD pattern of **SALI-25**, b) N_2 sorption isotherm of **SALI-25**.

16.

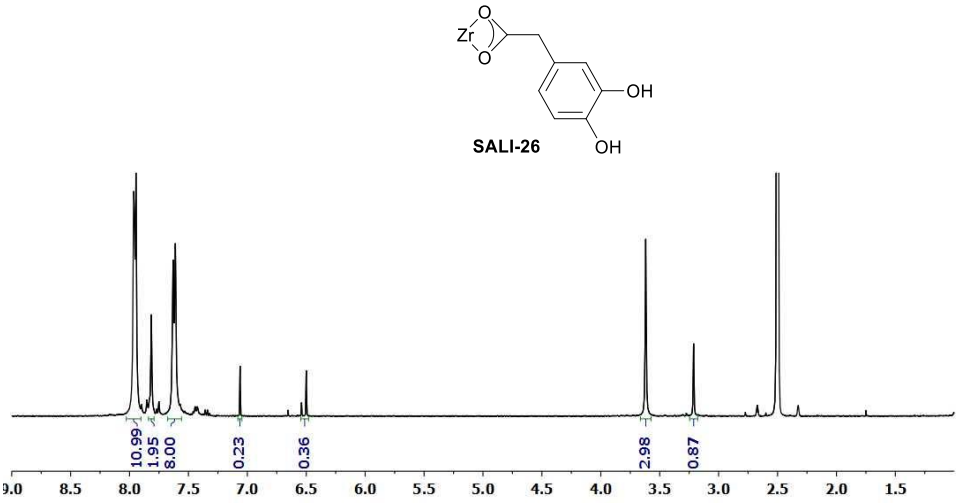

Figure S46. ^{1}H NMR of **SALI-26**.

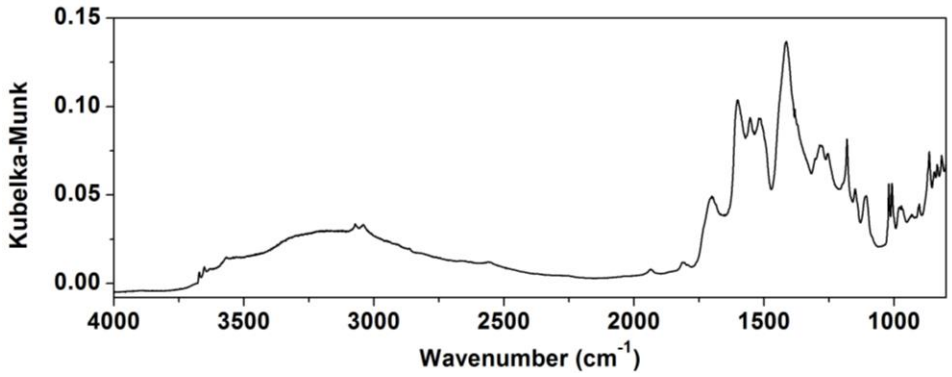

Figure S47. DRIFTS of **SALI-26**.

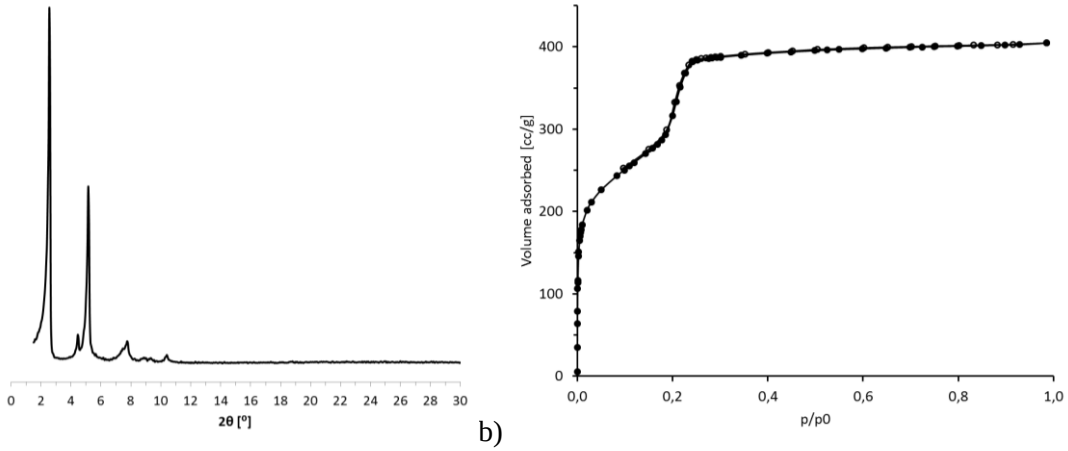

a) b)

Figure S48. a) PXRD pattern of **SALI-26**, b) N_2 sorption isotherm of **SALI-26**.

17.

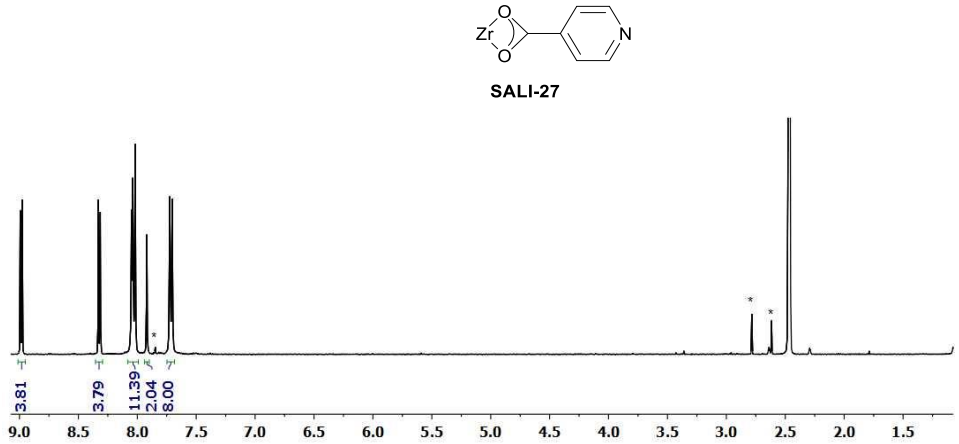

Figure S49. ^{1}H NMR of **SALI-27**. Solvent (DMF) peaks are marked with *.

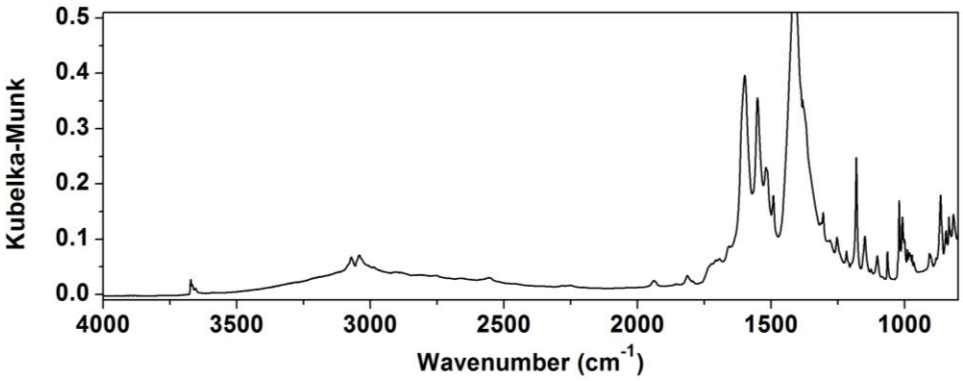

Figure S50. DRIFTS of **SALI-27**.

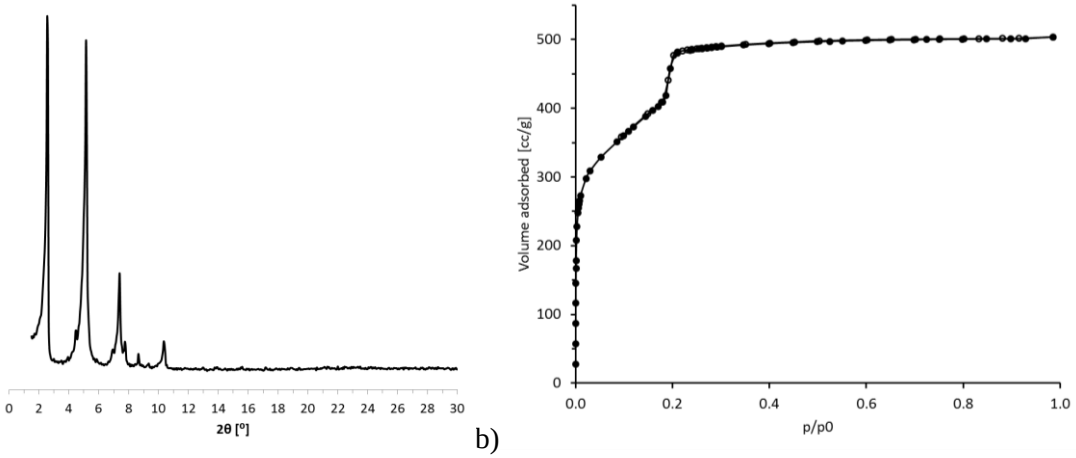

Figure S51. a) PXRD pattern of **SALI-27**, b) N_2 sorption isotherm of **SALI-27**.

18.

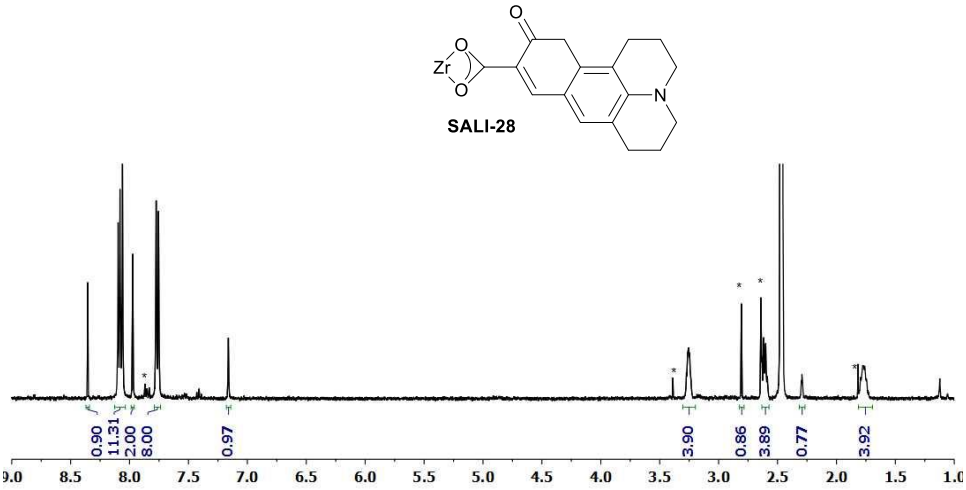

Figure S52. ^{1}H NMR of **SALI-28**. Solvent (DMF, MeCN) peaks are marked with *.

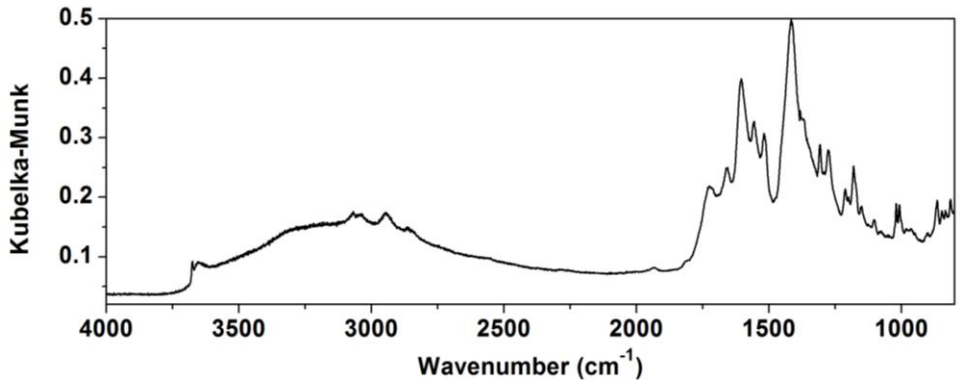

Figure S53. DRIFTS of **SALI-28**.

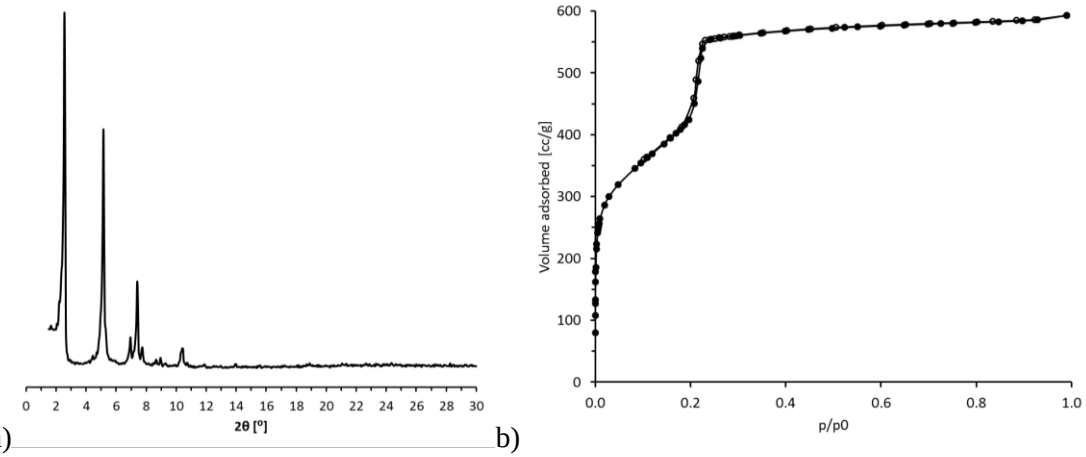

a) b)

Figure S54. a) PXRD pattern of **SALI-28**, b) N_2 sorption isotherm of **SALI-28**.

S4. Secondary reactions with SALI-n

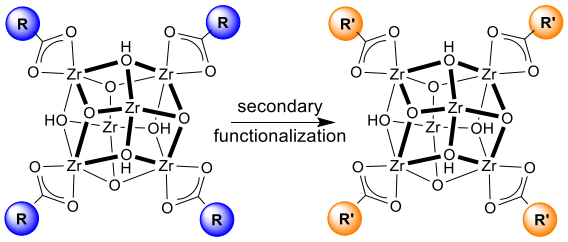

Scheme S2. Secondary functionalization of **SALI-n**.

S5A."Click" reaction with **SALI-25**

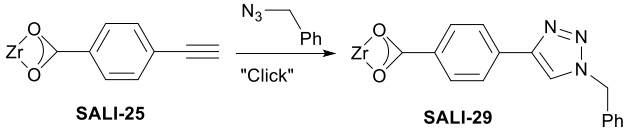

A 45 mg portion of activated **SALI-25** (0.02 mmol; ~0.06 mmol of **L15**) was loaded into a 5 mL microwave vial (Biotage) that contained a 2 mL portion of DMSO. Sodium ascorbate (4.7 mg, 0.024 mmol), benzyl azide (15 μL, 0.12 mmol) and $CuSO_4 \cdot 5H_2O$ (2mg, 0.012 mmol dissolved in 100 μL DMF) were subsequently added to the reaction vial, which was then sealed and heated at 60 ^{0}C for 3 h with occasional swirling. The MOF sample was then filtered, washed sequentially with DMSO, acetonitrile and dichloromethane (60, 40 and 30 mL each), and finally air dried. "Click" reaction yield: ~62%

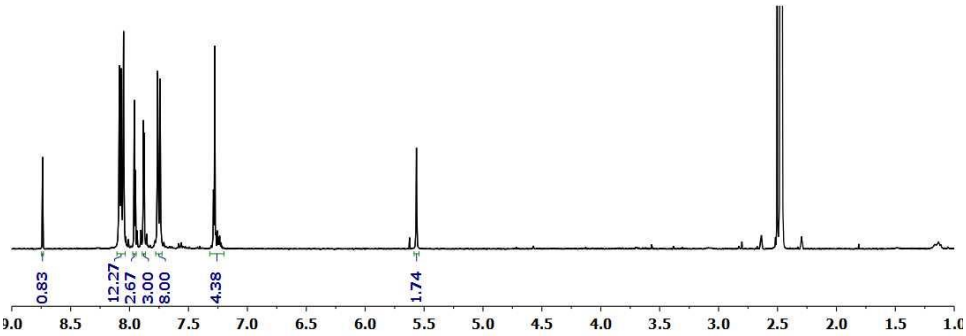

Figure S55. ^{1}H NMR of **SALI-29**.

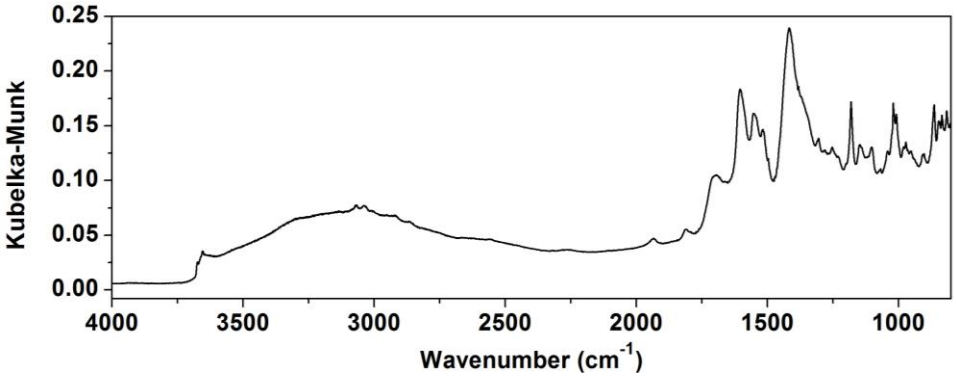

Figure S56. DRIFTS of **SALI-29**.

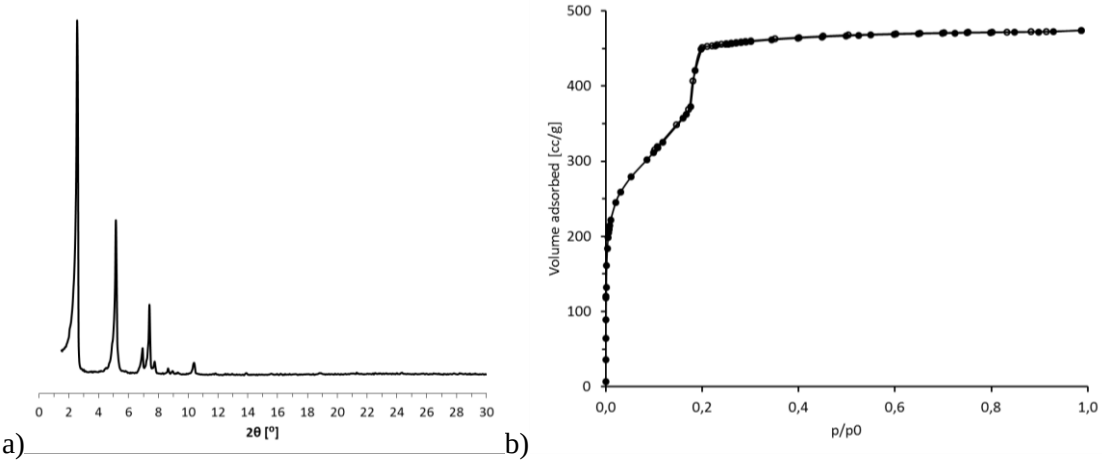

Figure S57. a) PXRD pattern of **SALI-29**, b) N_2 sorption isotherm of **SALI-29.**

S5B. "Click" reaction with **SALI-24**

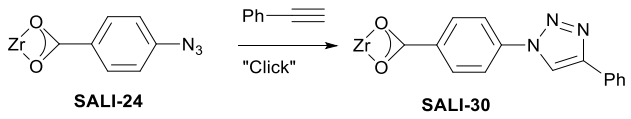

A 40 mg portion of activated **SALI-24** (0.022 mmol; ~0.09 mmol of **L14**) was loaded in a 5 mL microwave vial (Biotage) that contained a 2 mL portion of DMSO. Sodium ascorbate (1.80 mg, 0.009 mmol), phenylacetylene (12 μL, 0.10.9 mmol) and $CuSO_4 \cdot 5H_2O$ (0.72 mg, 0.0045 mmol dissolved in 72 μL DMF) were subsequently added to the reaction vial, which was then sealed and heated at 60 ^{0}C for 3 h with occasional swirling. The MOF sample was then filtered, washed sequentially with DMSO, acetonitrile and dichloromethane (60, 40 and 30 mL each), and finally air dried. "Click" reaction yield: ~60%.

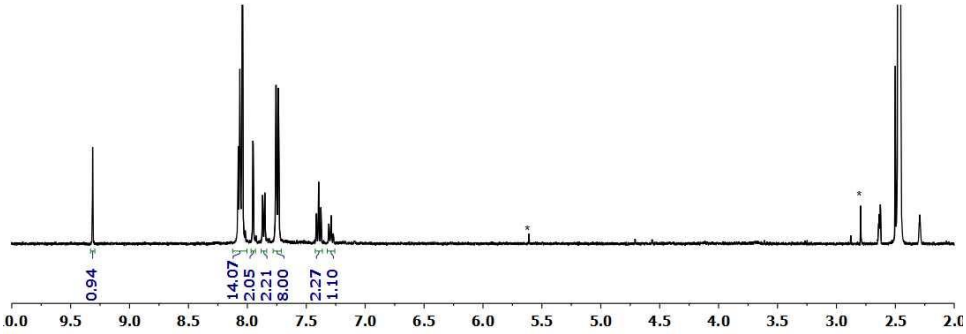

Figure S58. ^{1}H NMR of **SALI-30**. Solvent (DMF, DCM) peaks are marked with *.

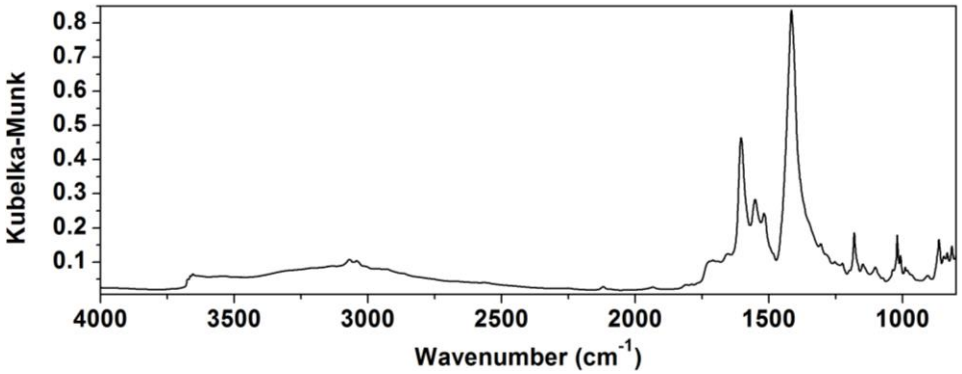

Figure S59. DRIFTS of **SALI-30**. Note that the azide stretching peak at 2123 cm^{-1} disappeared (see Figure S41).

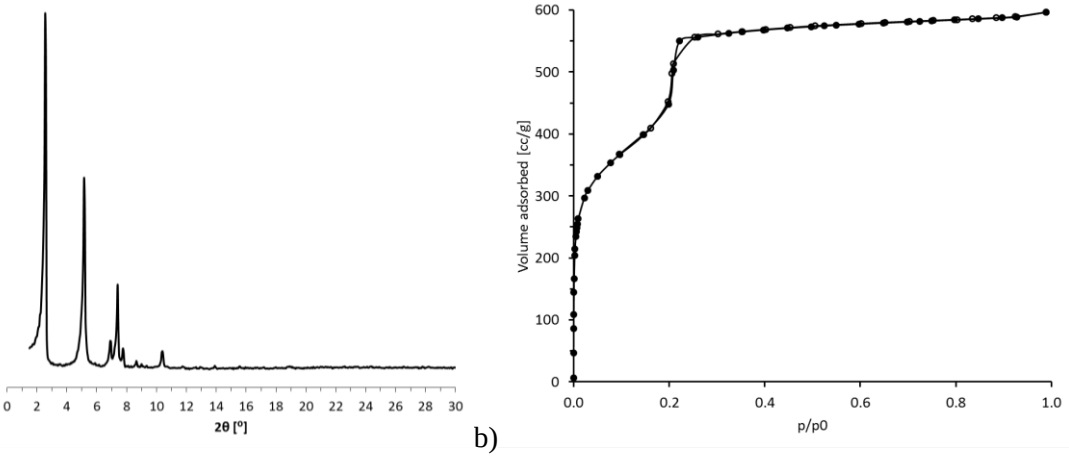

a) b)

Figure S60. a) PXRD pattern of **SALI-30**, b) N_2 sorption isotherm of **SALI-30.**

S5C. Imine condensation reaction with **SALI-21**

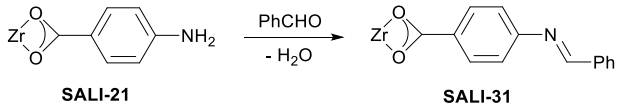

SALI-21 **SALI-31**

21 mg of activated **SALI-21** (0.009 mmol; ~0.018 mmol of **L11**) were loaded into a 5 mL microwave vial (Biotage) and 2 mL of ethanol were added. Benzaldehyde (36 µL, 0.36 mmol) was subsequently added to the reaction vial, which was then sealed and heated at 85 ^{0}C for 48 h with occasional swirling. The MOF sample was then filtered, washed 3 times with ethanol and dried at 120 °C under oil pump vacuum for 12 h yielding **SALI-31** material.

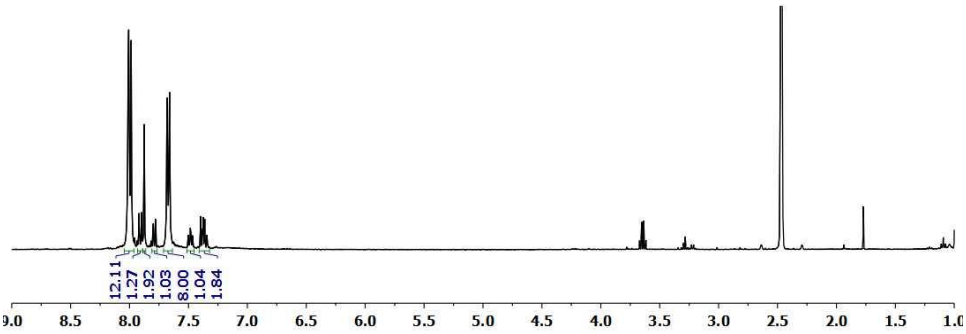

Figure S61. ^{1}H NMR of **SALI-31**.

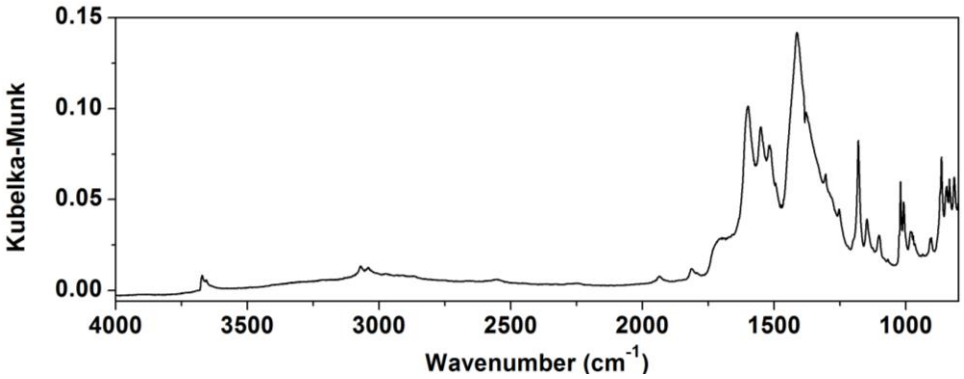

Figure S62. DRIFTS of **SALI-31**.

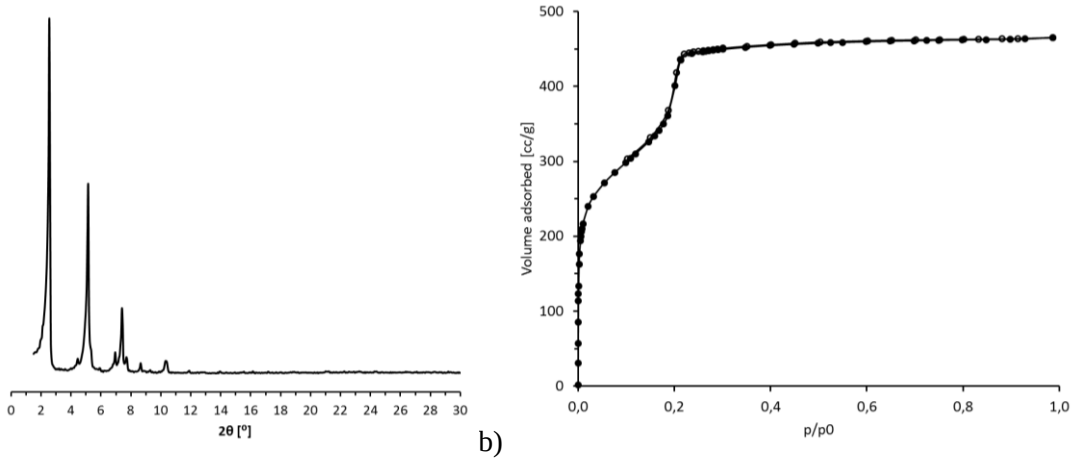

a) b)

Figure S63. a) PXRD pattern of **SALI-31**, b) N_2 sorption isotherm of **SALI-31.**

S5D.Methylation reaction with **SALI-27**

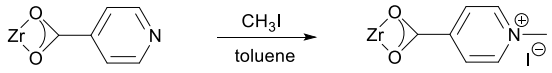

SALI-27 **SALI-32**

20 mg of activated **SALI-27** (0.008 mmol; ~0.016 mmol of **17**) were loaded into a 5 mL microwave vial (Biotage) and 2 mL of toluene were added. Methyl iodide (10 µL, 0.16 mmol) was subsequently added to the reaction vial, which was then sealed and heated at 85 ^{0}C for 48 h with occasional swirling. The MOF sample was then filtered, washed with toluene and then 3 times with acetone and dried at 120 °C under oil pump vacuum for 12 h yielding **SALI-32** material.

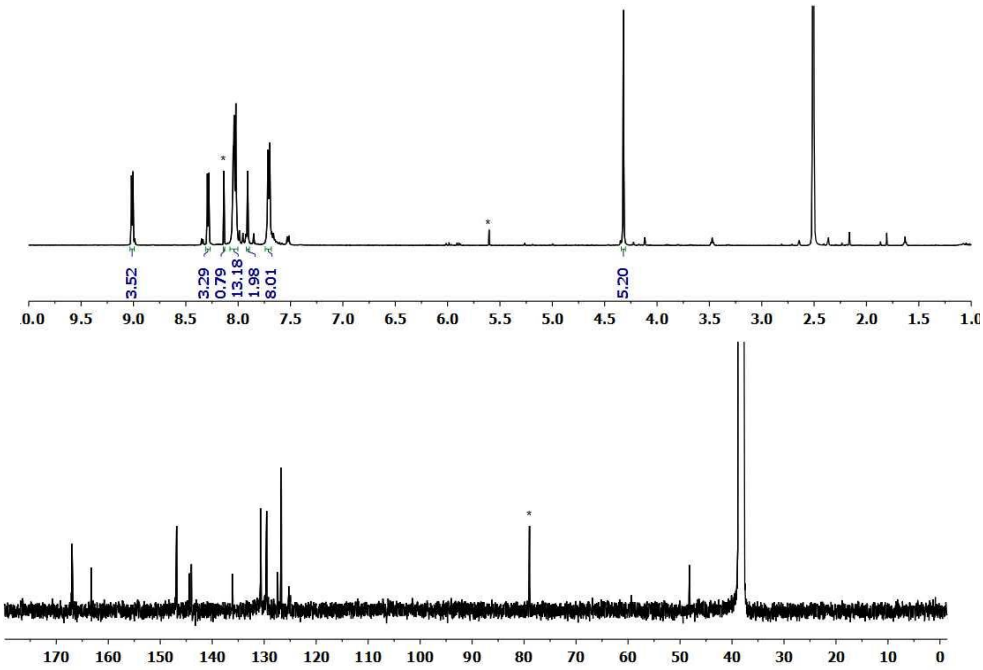

Figure S64. ^{1}H NMR (top) and ^{13}C NMR (bottom) of **SALI-32**. Solvents ($CHCl_3$ and CH_2Cl_2) peaks are marked with *.

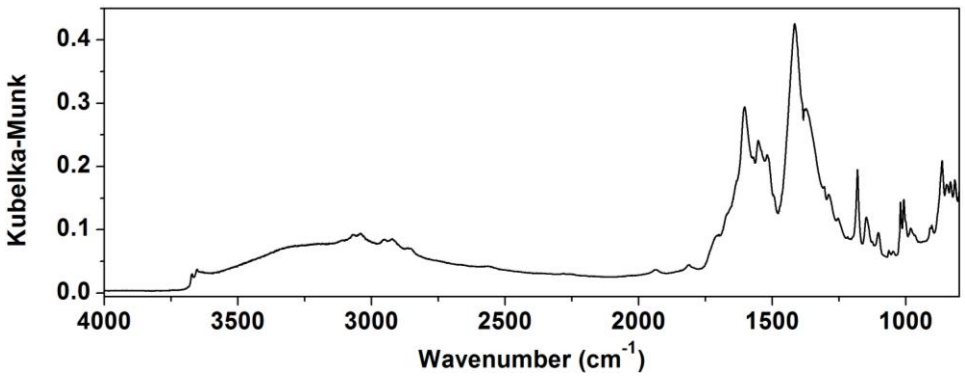

Figure S65. DRIFTS of **SALI-32**.

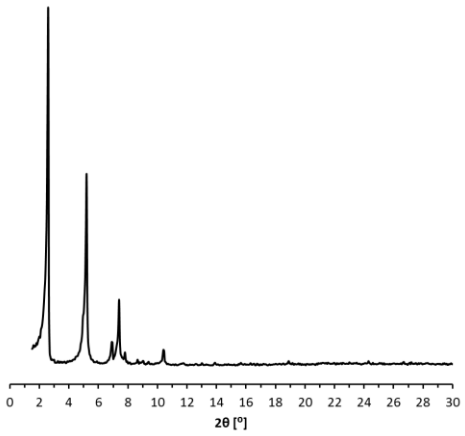

Figure S66. PXRD pattern of **SALI-32**.

S5. Conversion Rate of SALI-n

Depending on the identity of the CFG, between 2 and 4 CFGs were incorporated per Zr_6 node within **NU-1000** (Table S1). Higher ligand acidity (pK_a of the COOH of the incoming ligand) and lower ligand steric demand resulted higher in degrees of MOF functionalization. The maximum incorporation for each CFG ligand was established by placing the functionalized **SALI-n** material, obtained after 24h of reaction, into a fresh CFG solution for a second cycle of reaction of 24 h; in most cases the 2nd cycle did not result in higher incorporation. Likewise the rate of incorporation can also be expected to depend on the acidity and steric of incoming ligand. To further elucidate this point we choose pyridine-4-carboxilic acid (**L17**) to react with **NU-1000** as a function of time under similar condition. The ^{1}H NMR spectra of the resulting materials (**SALI-27**) indicate the conversion of **NU-1000** to **SALI-27** was complete within an hour time (**Figure S67**).

Rate of conversion for the secondary reactions were also estimated to be completed in 2-3 h time.

It should be noted that the time required recovering the solid **SALI-n** materials from the reaction mixture, either by filtration or centrifugation is about 10-15 min which adds a significant error when studying the reaction progress at a time point that is less than 1 h.

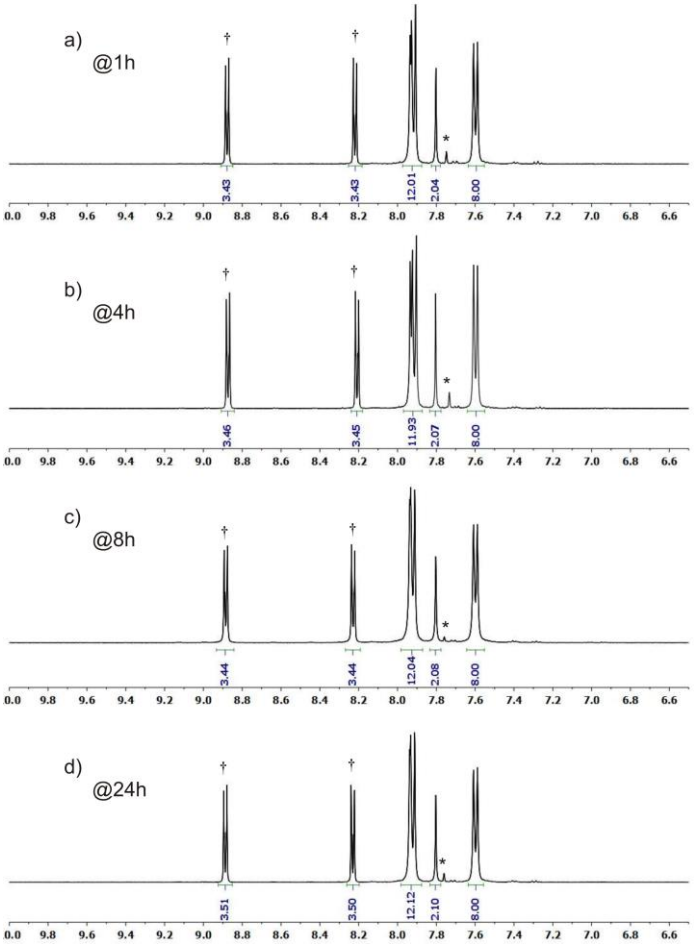

Figure S67. ^{1}H NMR spectra of **SALI-27** formation as a function of time during the reaction of **NU-1000** and **L17**. Peaks for **L17** and residual DMF solvent are marked with † and * respectively.

S6. Pore Size Distributions for NU-1000 and SALI-n.

The N_2 adsorption isotherms of the CFG - functionalized **SALI-n** samples show similar features as compared to the parent **NU-1000**: all N_2 adsorption isotherms are type IVc. Brunauer-Emmett-Teller (BET) analyses of the isotherms (Table S1) indicate a decrease in surface area from 2315 m^2/g for **NU-1000** to 600-1750 $m^2\ g^{-1}$ for **SALI-n** samples depending on the degree of incorporation and the steric hindrance of the CFG. Likewise, the pore size distribution was calculated using Barrett-Joyner-Halenda method (BJH). The pore volumes (Table S1) were also decreased for **SALI-n** samples as a function of space occupied by the incorporated CFG ligands, i.e. depending on the degree of functionalization and size of the CFG. Figure S68 show a comparison of the isotherms and corresponding BJH pore size distributions for the parent **NU-1000** and two SALI derivatives, **SALI-18** (**NU-1000**/4-idobenzoic acid) and **SALI-27** (**NU-1000**/isonicotinic acid). Systematic decrease of the pores size can be observed.

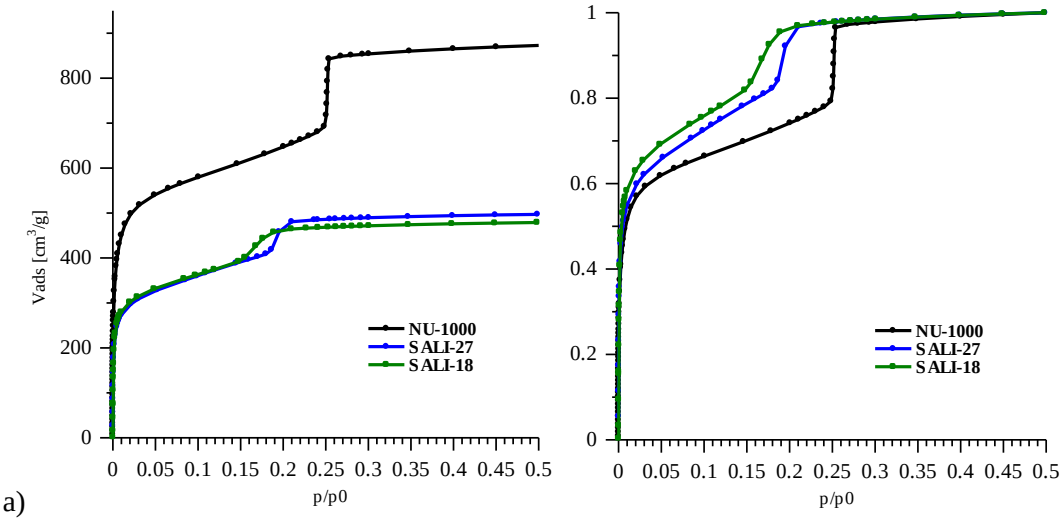

a)

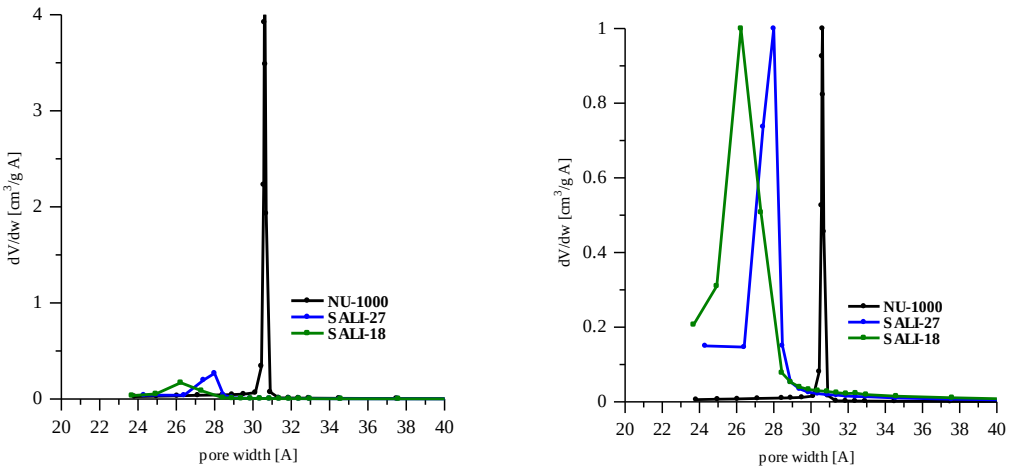

b) c)

Figure S68. Comparison of N_2 sorption data for **NU-1000**, **SALI-18** and **SALI-27**: a) as recorded (left) and normalized (right; with respect to the total uptake) adsorption isotherms; b) BJH pore size distribution calculated from desorption branch; c) normalized BJH pore size distribution showing change in the step @ ~0.22 P/P_0

S7. TGA for NU-1000 and SALI-n.

TGA data shows that the thermal stability of **SALI-n** materials mainly depends on the stability of the incorporated CFG ligand. For example, in case of **SALI-24** (**NU-1000**/4-azidobenzoic acid) decomposition of azido ligand takes place, similarly for **SALI-32** (**NU-1000**/(MeI×isonicotinic acid)) weight loss at 150 °C can observed due two the removal of MeI.

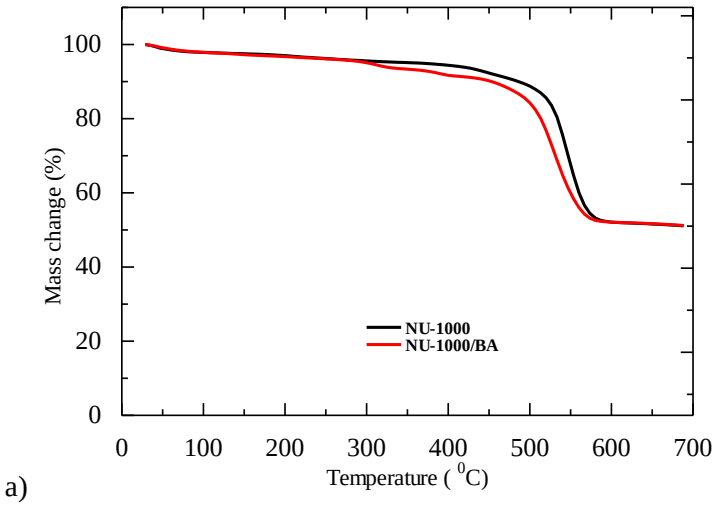

a)

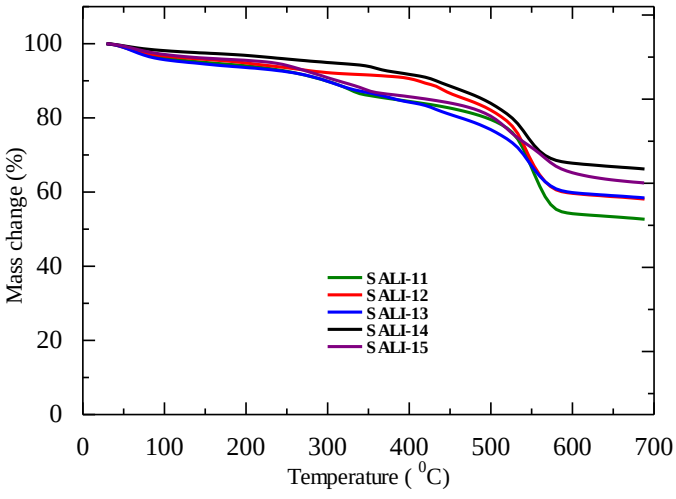

b)

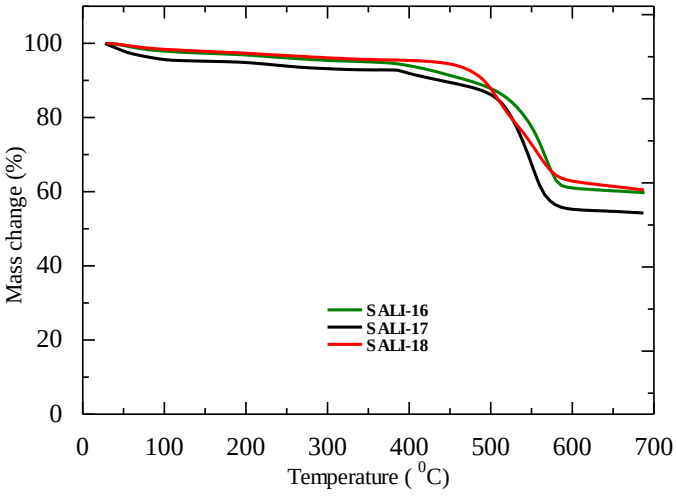

c)

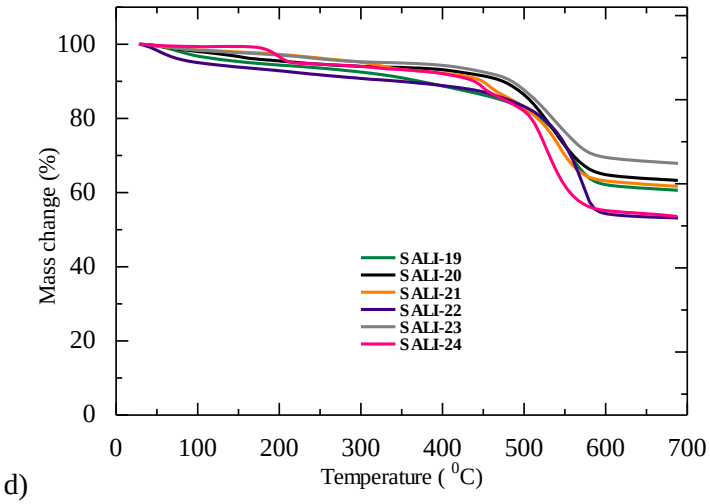

d)

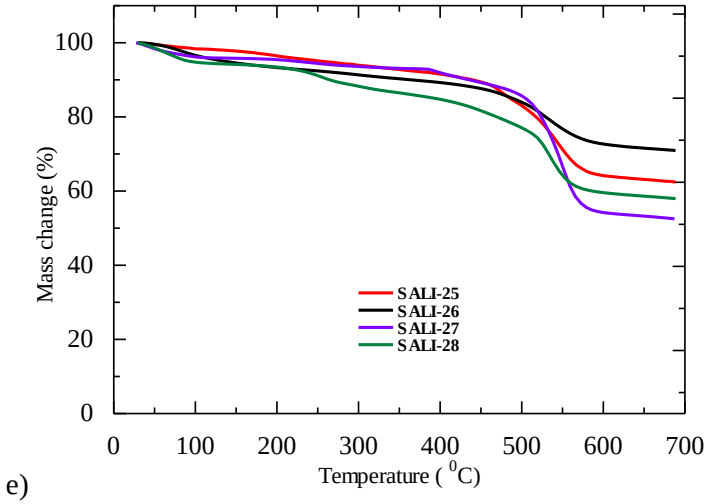

e)

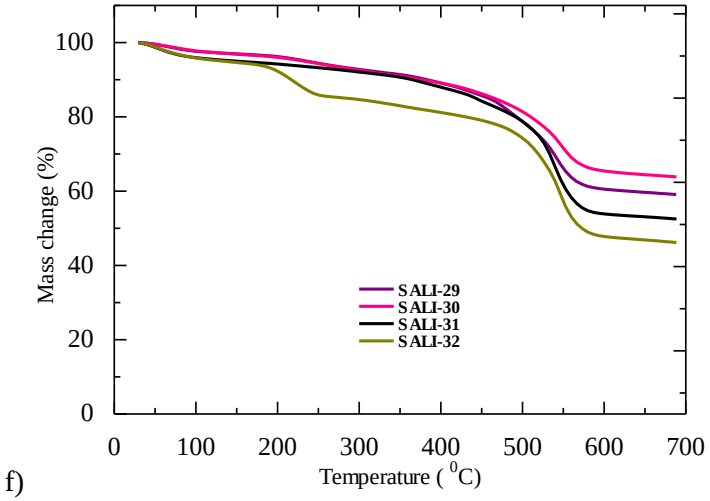

f)

Figure S69. TGA profiles for: a) the parent **NU-1000** and **NU-1000/BA**; b) **SALI-11** – **SALI-15**; c) **SALI-16** – **SALI-18**; d) **SALI-19** – **SALI-24**; e) **SALI-25** – **SALI-28**; f) **SALI-29** – **SALI-32**.

S8. References

(1) Mondloch, J. E.; Bury, W.; Fairen-Jimenez, D.; Kwon, S.; DeMarco, E. J.; Weston, M. H.; Sarjeant, A. A.; Nguyen, S. T.; Stair, P. C.; Snurr, R. Q.; Farha, O. K.; Hupp, J. T. *J. Am. Chem. Soc.* **2013**, *135*, 10294.
(2) Rouquerol, J.; Llewellyn, P.; Rouquerol, F. *Stud. Surf. Sci. Catal.* **2007**, *160*, 49.
(3) Walton, K. S.; Snurr, R. Q. *J. Am. Chem. Soc.* **2007**, *129*, 8552.